# Supplementary document: Patterns and determinants of the global herbivorous mycobiome

Casey H. Meili[1], Adrienne L. Jones[1], Alex Arreola[1], Jeff Habel[1], Carrie J. Pratt[1], Radwa A. Hanafy[1], Yan Wang[2], Aymen S. Yassin[3], Moustafa A. TagElDein[3], Christina D. Moon[4], Peter H. Janssen[4], Mitesh Shrestha[5], Prajwal Rajbhandari[5], Magdalena Nagler[6], Julia M. Vinzelj[6], Sabine M. Podmirseg[6], Jason E. Stajich[7], Arthur L. Goetsch[8], Jerry Hayes[8], Diana Young[9], Katerina Fliegerova[10], Diego Javier Grilli[11], Roman Vodička[12], Giuseppe Moniello[13], Silvana Mattiello[14], Mona T. Kashef[2], Yosra I. Nagy[2], Joan A. Edwards[15], Sumit Singh Dagar[16], Andrew P. Foote[17], Noha H. Youssef[1*], Mostafa S. Elshahed[1*]

[1] Oklahoma State University, Department of Microbiology and Molecular Genetics, Stillwater, Oklahoma, USA.
[2]Department of Biological Sciences, University of Toronto Scarborough, Toronto, Ontario, Canada.
[3] Department of Microbiology and Immunology, Faculty of Pharmacy, Cairo University, Cairo, Egypt.
[4]AgResearch, Grasslands Research Centre, Palmerston North, New Zealand.
[5]Department of Applied Microbiology and Food Technology, Research Institute for Bioscience and Biotechnology (RIBB), Kathmandu, Nepal.
[6]Universität Innsbruck, Faculty of Biology, Department of Microbiology, Innsbruck, Austria.
[7]Department of Microbiology and Plant Pathology, University of California, Riverside, Riverside, CA, USA
[8]Langston University, Langston, Oklahoma, USA.
[9]Bavarian State Center for Agriculture, Freising, Germany.
[10]Institute of Animal Physiology and Genetics Czech Academy of Sciences, Prague, Czechia.
[11]Área de Microbiología, Facultad de Ciencias Médicas, Universidad Nacional de Cuyo, Mendoza, Argentina
[12]Prague Zoo, Prague, Czechia.
[13]Department of Veterinary Medicine, University of Sassari, Sardinia, Italy.
[14]University of Milan, Dept. of Agricultural and Environmental Sciences, Milan, Italy.
[15] Anaerobic Fungi Network, Kerkdriel, Netherlands
[16]Bioenergy Group, Agharkar Research Institute, Pune, India.
[17]Department of Animal and Food Sciences, Oklahoma State University, Stillwater, Oklahoma, USA.

*Corresponding author: Address 1110 S. Innovation way, Stillwater, OK. Email: Mostafa@Okstate.edu and Noha@Okstate.edu

## I. Supplementary materials and methods

**Sampling.** A total of 661 samples belonging to thirty-four different mammalian animal species and nine families of foregut ruminant, foregut pseudoruminant, and hindgut fermenters were included in the final analysis (Figures 1a-b, Table S2). Samples were obtained from 15 different laboratories using a standardized procedure. Fresh, moist fecal samples originating from a single animal were scooped immediately post-defecation into sterile 50-ml plastic tubes and rapidly sealed. Samples were transferred to the laboratory on ice, usually within one hour, and stored at -20ºC prior to DNA extraction. All individuals collecting samples from domesticated animals were owners or caretakers and were authorized and trained in animal keeping and husbandry. For domesticated animals reared in a research institution, all IRB protocols for animal rearing were observed. Sampling wild herbivores was conducted through a partnership with hunting communities, alleviating the need for obtaining hunting permits. All hunters had the appropriate licenses, and the animals were shot on public land during the hunting season.

**DNA extraction.** DNA extractions were conducted in eight laboratories (Oklahoma, USA: 418 samples, Egypt: 74 samples, Nepal: 25 samples, Austria: 10 samples, Italy:38 Samples, Czechia: 24 samples, Germany: 31 samples, and New Zealand: 35 samples) and followed the manufacturer's instructions for DNeasy Plant Pro Kit (Qiagen®, Germantown, Maryland). Few samples were from a prior study [1]. The kit was shipped from the USA to labs in Nepal and Egypt and was purchased independently elsewhere.

**PCR amplification, and Illumina sequencing.** The 28S rRNA was used as the phylomarker for this diversity survey since as previously suggested for AGF genus-level delineation [2, 3]. The LSU rRNA has been regarded as a more reliable marker for AGF diversity characterization (compared to the general fungal phylomarker ITS1 region) by the scientific community [4], and has been

previously employed in AGF culture-independent diversity surveys [5]. By comparison, the ITS1 region suffers from high within-strain sequence divergence, and length variability [5, 6]. All PCR amplifications were conducted in a single laboratory to eliminate inter-laboratory variability. All reactions utilized the DreamTaq Green PCR Master Mix (ThermoFisher, Waltham, Massachusetts), and primers targeting the D2 region of the LSU rRNA (AGF-LSU-EnvS For: 5'-GCGTTTRRCACCASTGTTGTT-3', AGF-LSU-EnvS Rev: 5'-GTCAACATCCTAAGYGTAGGTA-3') for amplification. The primers were recently developed and extensively evaluated for sensitivity, specificity, Neocallimastigomycota coverage, and ability to differentiate between all known AGF genera and candidate genera [7]. The primers target a ~370 bp region of the LSU rRNA gene (corresponding to the D2 domain), hence allowing for high throughput sequencing using the Illumina MiSeq platform. Primers were modified to include the Illumina overhang adaptors. PCR reactions contained 2 µl of DNA, 25 µl of the DreamTaq 2X master mix (Life Technologies, Carlsbad, California), and 2 µl of each primer (10 µM) in a 50 µl reaction mix. The PCR protocol consisted of an initial denaturation for 5 min at 95 °C followed by 40 cycles of denaturation at 95 °C for 1 min, annealing at 55 °C for 1 min and elongation at 72 °C for 1 min, and a final extension of 72 °C for 10 min. PCR products were individually cleaned to remove unannealed primers using PureLink® gel extraction kit (Life Technologies, Carlsbad, California), and the clean product was used in a second PCR reaction to attach the dual indices and Illumina sequencing adapters using Nexterra XT index kit v2 (Illumina Inc., San Diego, California). These second PCR products were then cleaned using PureLink® gel extraction kit (Life Technologies, Carlsbad, California), individually quantified using Qubit® (Life Technologies, Carlsbad, California), and pooled using the Illumina library pooling calculator (https://support.illumina.com/help/pooling-calculator/pooling-calculator.htm)

to prepare 4-5 nM libraries. Pooled libraries (300-350 samples) were sequenced at the University of Oklahoma Clinical Genomics Facility using the MiSeq platform.

**Complementary PacBio sequencing.** The 700-750 bp D1/D2 LSU fragment has recently been adopted [4] as the gold standard for AGF genus- and species-level assignments, as well as for circumscribing boundaries between various AGF clades. However, the length of the region precludes the use of Illumina technology for high throughput sequencing and necessitates the use of the technically more cumbersome and expensive Sanger or PacBio sequencing platforms. Therefore, as a complementary approach to Illumina sequencing, we conducted PacBio sequencing on a subset of the Illumina-sequenced samples (n=61) with the following goals in mind: (1) to ensure that community membership, structure, and diversity estimates obtained with the shorter fragment (D2 region only) are comparable to those obtained with the previously utilized D1/D2 region, (2) to ensure the feasibility and resolution power of the D2 region in identifying and differentiating various fungal lineages, and (3) to confirm the presence of the unexpectedly high number of putative novel genera, provide full-length representative sequences [4], and amend the curated D1/D2 LSU rRNA database currently handled by the authors as part of the broader AGF community of researchers (www.anaerobicfungi.org). For amplification of the D1/D2 LSU region, we paired a universal fungal forward primer (NL1: 5'-GCATATCAATAAGCGGAGGAAAAG-3') with an AGF-specific reverse primer (GG-NL4: 5'-TCAACATCCTAAGCGTAGGTA-3') [5, 8]. Primers were barcoded to allow multiplexing and PacBio sequencing. The PCR protocol consisted of an initial denaturation for 5 min at 95 °C followed by 40 cycles of denaturation at 95 °C for 1 min, annealing at 55 °C for 1 min and elongation at 72 °C for 1 min, and a final extension of 72 °C for 10 min. Amplicons were purified using PureLink® gel extraction kit (Life Technologies), quantified using Qubit® (Life

Technologies), pooled, and sequenced at Washington State University core facility using one cell of the SMRT Pacific Biosciences (PacBio) Sequel II system.

**Illumina and PacBio sequence processing:** Forward and reverse Illumina reads were assembled using make.contigs command in mothur [9], followed by screening to remove sequences with ambiguous bases, sequences with homopolymer stretches longer than 8 bases, and sequences that were shorter than 200 or longer than 380 bp. For PacBio sequences, raw reads were processed using the official PacBio pipeline (RS_Subreads.1) (http://files.pacb.com/software/smrtanalysis/2.2.0/doc/smrtportal/help/!SSL!/Webhelp/CS_Prot_RS_Subreads.htm), and filtered using default settings of the minimum read length, and minimum read quality. Remaining reads were then processed with the PacBio RS_ReadsOfInsert protocol (http://files.pacb.com/software/smrtanalysis/2.2.0/doc/smrtportal/help/!SSL!/Webhelp/CS_Prot_RS_ReadsOfInsert.htm) for generating single-molecule consensus reads from the insert template. Circular consensus sequences were further processed in mothur [9] to remove any sequence with an average quality score < 25, sequences with ambiguous bases, sequences not containing the correct barcode, sequences with more than a 2 bp difference in the primer sequence, and/or sequences with homopolymer stretches longer than 8 bp. To identify any CCS with the primer sequence in the middle, we performed a standalone blastn-short using the primer sequence as the query and removed the identified sequences using the remove.seqs command in mothur.

**Taxonomic and phylogenetic assignments.** To examine how taxa delineation cutoffs previously proposed based on the D1/D2 region [4, 5] correlate to those of the shorter Illumina-generated D2 LSU fragments obtained in this study, we conducted preliminary comparison of all possible pairwise sequence divergence values from the alignment of the whole D1/D2 region of 206 reference sequences (available at www.anaerobicfungi.org), to those from the truncated

alignment covering the D2 region only (corresponding to the region that would be amplified using the AGF-LSU-EnvS primer pair above). Sequence divergence estimates from the two sets of alignments were very well correlated ($R^2$= 0.885, Figure S9). However, comparison of pairwise sequence divergence using the whole D1/D2 region versus the D2 region suggests that the 2% sequence divergence cutoff previously proposed as the threshold for delineating AGF species using the D1/D2 region (based on comparisons of validly described species) [4] is equivalent to 3.5% using the D2 region only, and the 3% sequence divergence cutoff previously proposed as the threshold for delineating AGF genera using the D1/D2 region [4] is equivalent to 5.1% using the D2 region only (Figure S9).

Therefore, pairwise distances were used to cluster the sequences into species-level OTUs using the proposed sequence threshold of 3.5%. On the other hand, prior research has shown that using specific thresholds for genus-level delineation in AGF is problematic. For example, some genera were found to harbor higher intra-genus D1/D2-LSU region sequence divergence values (e.g. the genus *Piromyces* intra-genus D1/D2-LSU region sequence divergence ranges between 0% and 5.7%), while others diverge by <2% from neighboring genera (e.g. the *Anaeromyces-Liebetanzomyces-Capellomyces-Oontomyces* clade harbors inter-genus D1/D2-LSU region sequence divergence values ranging between 1.8% and 2.5%) [4]. Therefore, we refrained from using a predetermined threshold to assign sequences to AGF genera and instead used a two-tier approach for genus-level phylogenetic placement. First, sequences were compared by blastn to the curated D1/D2 LSU rRNA AGF database (www.anaerobicfungi.org), and sequences were classified as their first hit taxonomy if the percentage similarity to the first hit was >96% and the two sequences were aligned over >70% of the query sequence length. For all sequences that could not be confidently assigned to an AGF genus by blastn, insertion into a reference LSU tree

(with representatives from all cultured and uncultured AGF genera and candidate genera) was used to assess novelty. Briefly, unaffiliated sequences (100-200 at a time) were aligned to the reference database using align.seqs in mothur, and the alignment was used to construct maximum likelihood phylogenetic trees in FastTree [10] using the GTR model. Sequences were assigned to a novel genus when they cluster as an independent genus-level clade with high (>70%) bootstrap support in the ML tree. Representatives of novel genera were sequentially added to the reference LSU tree, before processing the next batch of unaffiliated sequences. Intra-genus D2 region sequence divergence for sequences assigned to any novel genus never exceeded 5% (equivalent to 3% D1/D2 sequence divergence). Following the assignment of all sequences to either an existing or a novel genus, final trees with 5-10 representatives of each genus were generated in IQ-TREE [11] using the alignment of the D2 region. ModelFinder [12] through IQ-TREE was used to select the best substitution model (with the lowest Bayesian information criterion). Maximum likelihood trees were constructed under the predicted best model, with the -alrt 1000, the -bb 1000, and the --abayes options added to the commandline for performing the Shimodaira–Hasegawa approximate likelihood ratio test (SH-aLRT), the ultrafast bootstrap (UFB) [13], and the approximate Bayes test. This resulted in the generation of phylogenetic trees with three support values (SH-aLRT, aBayes, and UFB) on each branch. Phylogenetic analysis as described above resulted in the confident assignment of every single sequence to either an existing cultured, or uncultured genus, or to a novel genus. These genus-level assignments were then used to build a taxonomy file in mothur, which was subsequently used to build a shared file using the mothur commands phylotype and make.shared.

Amplicon sequence variants (ASVs) have recently been gaining popularity and momentum in describing diversity in bacterial [14, 15], archaeal [16], and fungal [17] surveys, a

proposition augmented by improved sequence quality and stringent quality control procedures on all sequencing platforms [18, 19, 20, 21], we, however, refrained from using ASVs in this study, due to the fact that a significant level of within-strain divergence (ranging between 0.1%-1.9% [5]) is observed in the multiple LSU rRNA gene copies (estimated around 170 per genome). As such, use of ASVs, with its emphasis on exact sequencing identity [18, 19, 20] would immensely overestimate AGF diversity and bias community structure estimates.

**Role of stochastic versus deterministic processes in shaping AGF community assembly.** We assessed the contribution of various deterministic and stochastic processes to the AGF community assembly using both normalized stochasticity ratio (NST) [22], and the null-model-based quantitative framework implemented by [23, 24]. The NST index infers ecological stochasticity, however, values do not pinpoint the sources of selection (determinism) or stochasticity. Also, NST values are calculated solely based on taxonomic diversity indices with no consideration to the phylogenetic turnover in the community. To quantify the contribution of various deterministic (homogenous and heterogenous selection) and stochastic (dispersal preference, limitation, drift) processes in shaping the AGF community assembly, we used a two-step null-model-based quantitative framework that makes use of both taxonomic ($RC_{Bray}$) and phylogenetic (βNRI) β-diversity metrics [23, 24]. The NST package in R was used to calculate the normalized stochasticity ratio (NST) based on two taxonomic β-diversity dissimilarity metrics; the incidence-based Jaccard index, and the abundance-based Bray-Curtis index, where an NST value of >50% indicates a more stochastic assembly, while values <50% indicate a more deterministic assembly. To test the significance of difference between pairs of animal species (for animals with more than 20 individuals; cows, goats, sheep, deer, and horses), animal families (for families with more than 10 individuals; Bovidae, Cervidae, Camelidae, Equidae,

196 and Elephantidae), and animal gut types (foregut, pseudoruminant, and hindgut), we used the
197 function nst.boot in the NST package in R to randomly draw samples within each group followed
198 by bootstrapping of NST values. Obtained values were then compared using Wilcoxon test with
199 Benjamini-Hochberg adjustment. The iCAMP R package was used to calculate values of beta net
200 relatedness index (βNRI) and modified Raup-Crick metric based on Bray Curtis metric ($RC_{Bray}$)
201 using the function bNRIn.p to evaluate the turnover for both phylogenetic, and taxonomic
202 diversity. Values of βNRI were used first to partition selective processes into homogenous
203 (number of pairwise comparisons with βNRI values <-2), and heterogenous selection (number
204 of pairwise comparisons with βNRI values >2). All other pairwise comparisons (with absolute
205 βNRI values <2) are considered as contributing to stochastic processes (not assigned to selection),
206 and can be further broken down into dispersal and drift based on the taxonomic diversity (values
207 of $RC_{Bray}$). Specifically for these, the number of pairwise comparisons with absolute values of
208 $RC_{Bray}$ <0.95 are considered as contributing to drift, while the number of pairwise comparisons
209 with absolute values of $RC_{Bray}$ >0.95 are considered contributing to dispersal. This last fraction
210 can be further broken down into homogenizing dispersal ($RC_{Bray}$ values <-0.95), and dispersal
211 limitation ($RC_{Bray}$ values >0.95). The contribution of each of these processes (homogenous
212 selection, heterogenous selection, homogenizing dispersal, dispersal limitation, and drift) to the
213 total AGF community assembly was calculated from the corresponding number of pairwise
214 comparisons falling into each category as a percentage of all pairwise comparisons.
215 **Factors impacting AGF diversity and community structure.** We considered two types of
216 factors that could potentially impact AGF diversity and community structure: host-associated
217 factors, and non-host-associated factors. For host-associated factors, we considered animal
218 species, animal family, and animal gut type, while for non-host-associated factors, we considered

219 animal domestication status, biogeography (country of origin), animal age, and animal sex. For
220 testing the effect of biogeography, age, and sex on alpha diversity measures and community
221 structure, we opted to carry out comparisons only on samples belonging to the same animal
222 species in an attempt to control for other host-associated factors that might conflate the results.
223 For these comparisons, only the four most-sampled animal species (cattle, goats, sheep, and
224 horses) were considered.
225 **Alpha diversity measures.** Alpha diversity estimates (observed number of genera, Shannon,
226 Simpson, and Inverse Simpson diversity indices) were calculated using the command
227 estimate_richness in the phyloseq R package. For comparison of alpha diversity between
228 samples, patterns were assessed in samples with at least 1000 sequences (n=421 samples) using
229 the four indices, and two sampling strategies (with and without random subsampling of 1000
230 sequences) for eight total comparisons. The importance of various factors (host-associated
231 factors, e.g., gut type, animal family, or animal species; domestication status, and biogeography)
232 in shaping the observed patterns of alpha diversity was examined using ANOVA (calculated
233 using the aov command in R). Only samples that have at least 10 replicates (at any of these host
234 factor levels) were included in the analysis. These included foregut and hindgut (for the gut type
235 factor comparison), families Bovidae, Cervidae, and Equidae (for the animal family
236 comparison), cows, goats, sheep, deer, and horses (for the animal genus comparison), and
237 domesticated and non-domesticated (for domestication status comparison). Additionally, post
238 hoc Tukey HSD tests for multiple comparisons of means were run on the results of ANOVA
239 (using TukeyHSD command in R) for all possible pairwise comparisons to identify the pairs of
240 groups that are significantly different for each host factor.
241 As mentioned above, we opted to carry out comparisons of the effect of biogeography,

age, and sex only on samples belonging to the same animal species (only the four most-sampled animals were included) in an attempt to control for other host-associated factors that might conflate the results. Biogeography comparisons were conducted on cattle, goat, sheep, and horse datasets originating from the USA, Egypt, Germany, Italy, Austria, Czech Republic, New Zealand, and Argentina. ANOVA (calculated using the aov command in R) was used to identify the animal species whose AGF alpha diversity significantly differed between countries. For these animal datasets, post hoc Tukey HSD tests for multiple comparisons of means were run on the results of ANOVA (using TukeyHSD command in R) for all possible pairwise country comparisons to identify the pairs that are significantly different for each animal genus. Additionally, the effect of the US state of origin on AGF alpha diversity in cattle and horses was also tested using ANOVA followed by post hoc Tukey HSD tests for multiple comparisons of means for all possible pairwise state comparisons to identify the pairs that are significantly different for each animal species.

Age (young, <1 year; adult, >1 year), and sex (male versus female) comparisons were also considered only for the four most-sampled animals (cattle, goats, sheep, and horses). ANOVA followed by post hoc Tukey HSD tests were used.

**AGF community structure.** The genus-level shared file was used to calculate several beta diversity indices (including the phylogenetic similarity-based (e.g. unweighted and weighted Unifrac) using the ordinate command in the phyloseq R package. The pairwise values were used to construct ordination plots (both PCoA and NMDS) using the function plot_ordination in the phyloseq R package. RDA plots were also constructed using the genera abundance data following center log-ratio transformation (CLR). To assess the variability in community structure between samples belonging to each animal host species (only for animals with 4 or more

individuals), animal host family, animal gut type, and animal domestication status, we first calculated group centroids for each of these groups using the vegan command betadisper. Following, the ordination distance of each sample to its group centroid was calculated (as the Euclidean distance between two points), and distances from group centroids were plotted in a box and whisker plot (using the command boxplot in R). To partition the dissimilarity among the sources of variation (including animal host species, animal host family, animal gut type, and domestication status), PERMANOVA tests were run for each of the above beta diversity measures using the vegan command adonis, and the F-statistics p-values were compared to identify the host factors that significantly affect the AGF community structure. The percentage variance explained by each factor was calculated as the percentage of the sum of squares of each factor to the total sum of squares.

Due to the inherent sensitivity of PERMANOVA to the heterogeneity of variance among groups [25], and to further quantitatively assess factors that explain AGF diversity, we used three multivariate regression approaches based on matrices comparison: multiple regression of matrices (MRM), Mantel tests for matrices correlations, and Procrustes rotation. Bray-Curtis, and Jaccard dissimilarity matrices were first calculated from the genus shared file using vegdist command in vegan. Similarly, Unifrac weighted, and Unifrac unweighted dissimilarity matrices were calculated using the distance command in the phyloseq package. Each of these four AGF dissimilarity matrices were compared to a matrix of each of the host factors tested (animal host species, animal host family, animal gut type, and domestication status). For the animal host genus, a cophenetic matrix was calculated (using the command cophenetic in the ape R package) based on the newick tree downloaded from timetree.org and modified to include all the samples studied here with very short branch length between samples from the same animal species. For

288 the animal host family, animal gut type, and domestication status, since these were nominal
289 values, matrices were constructed by Gower transformation [26]. Each of the AGF community
290 dissimilarity matrices (n=4) was then correlated to each of the host factor matrices (n=4) using
291 the commands MRM, and mantel in the ecodist R package, for running multiple regression on
292 matrices, and Mantel tests, respectively. The Procrustes rotation was calculated using the protest
293 command in the vegan R package. For each of the host factors tested, 12 total correlations (3
294 methods x 4 dissimilarity indices) were compared to evaluate the importance of the host factor in
295 explaining the AGF community structure. This was achieved by comparing the p-values for
296 significance of correlation, and coefficients ($R^2$ regression coefficients of the MRM analysis,
297 Spearman correlation coefficients of the Mantel test, and symmetric orthogonal Procrustes
298 statistic of the Procrustes analysis) for the importance of the factor in explaining community
299 structure. Finally, to assess the sensitivity of multivariate regression methods to community
300 composition variation among hosts of the same species, we permuted the MRM analysis 100
301 times, where one individual per animal species was randomly selected. For each of these
302 permutations, and for each dissimilarity matrix-host factor comparison, a p-value and an $R^2$
303 regression coefficient were obtained. We considered a host factor significant in explaining AGF
304 community structure, if in the permutation analysis, the p-value obtained was significant ($p < 0.05$)
305 in at least 75 permutations.
306 To test for the effect of biogeography, sex, and age on the AGF community structure, and
307 to overcome compounded effects from other host factors, we selected a subset of the whole
308 dataset to include only samples from the four most-sampled animals (namely, cattle, goats,
309 sheep, and horses). For each of these animal species, we calculated Bray-Curtis dissimilarity
310 indices using the ordinate command in the phyloseq R package. To test for the significance of

311 the above three factors in describing AGF community structure in each animal genus,
312 PERMANOVA tests were run using the vegan command adonis. The F-statistics p-value was
313 used to assess the significance of AGF community difference between countries, young versus
314 adult animals, and males versus females, and the sum of squares was used to assess the
315 percentage variance explained by the country of origin for each of the four animal species.
316 Additionally, RDA plots were also constructed using the genera abundance data following center
317 log-ratio transformation (CLR).
318 **Assessing phylosymbiosis patterns.** To test for patterns of phylosymbiosis and the presence of
319 a cophylogenetic signal between the animal host and the AGF genera constituting the gut
320 community, we used Procrustes Application to Cophylogenetic Analysis (PACo) through the
321 paco R package. Briefly, the analysis involves the host cophenetic distance matrix (reflecting the
322 phylogenetic relationships between hosts), the AGF cophenetic distance matrix based on the
323 phylogenetic relationship of the different AGF genera to each other, and the AGF genera
324 abundance in the samples. With these three inputs, the analysis then translates the distance
325 matrices of the animal host and the AGF phylogenies into principal coordinates, followed by
326 rotating one set of the coordinates to maximize superimposition on the other. The sum of squared
327 residuals of this superimposition was calculated and used as an indication of congruency
328 between the two sets, with a smaller sum of squared residuals indicating better congruency. A
329 bias-correction step was also added. The analysis produces, besides the bias-corrected sum of
330 squared residuals, a p-value for the goodness of fit between the two phylogenies. Additionally, to
331 assess the sensitivity of PACo analysis to community composition variation among hosts of the
332 same species, we repeated the analysis while subsampling one individual per host genus (n=100
333 subsamples) and compared the distribution of PACo Procrustes residuals of the sum of squared

differences between different animal species, different animal families, and different gut types. To test for the significance of the difference between residuals, we used Wilcoxon test with Benjamini-Hochberg adjustment.

For pinpointing specific animal host-fungal associations, we employed two approaches. We first used the phyloSignal command in the phylosignal R package to calculate three global phylogenetic signal statistics, Abouheif's Cmean, Moran's I, and Pagel's Lambda. The values of these statistics plus the associated p-values identify the AGF genera that have a significant association with an animal host. We considered any genus with p-value $< 0.05$ with at least one statistic to be significantly correlated to the host phylogenetic tree. We then used the lipaMoran command in the phylosignal R package to calculate Local Indicator of Phylogenetic Association (LIPA) values for each sample-AGF genus pair, along with the associated p-values of association significance. For AGF genera showing significant associations (LIPA p-values $<0.05$), we calculated average LIPA values for each animal host species, and animal family. We considered average LIPA values in the range of 0.2-0.4 to represent weak associations, in the range 0.4-1 to represent moderate associations, and above 1 to represent strong associations.

To further explore the notion that enrichments of an ensemble of multiple genera, rather than a single genus, is responsible for the distinct community structure observed in foregut fermenters, we constructed a double principal coordinate analysis (DPCoA) ordination using the genera with abundance in the top 25% in each sample and that occurred in at least 50% of the samples. The genera (n=28) were first selected using the filterfun_sample(topp(0.25)) command in phyloseq followed by pruning the dataset using the genefilter_sample command. The DPCoA was constructed using the ordinate command in phyloseq followed by plot_ordination. DPCoA uses both abundance and phylogenetic information about the samples, allowing both the samples

and the taxa to be plotted on the same coordinate space, and thus the Euclidean distance between samples or their group centroids and AGF genera could be compared. Thus, AGF genera with Euclidean distances close to group centroids are considered to contribute more to the community structure of the group. We used betadisper in the R package vegan to calculate centroids for the three different gut types, the nine different animal families, and the animal genera with at least 4 individuals (n=15), and ggplot2 to draw 95% confidence level ellipses for the three gut types.

**Transcriptomic analysis.** Prior studies by our research group have generated 21 transcriptomes from 7 genera [27, 28]. Here, we added 20 transcriptomes from 7 additional genera, isolated during a long-term multi-year isolation effort in the authors' laboratory [4, 29] and included an extra 11 publicly available transcriptomic datasets [30, 31, 32, 33]. Cultures grown in rumen fluid-cellobiose medium [34] were vacuum filtered and then grounded with a pestle under liquid nitrogen. Total RNA was extracted using an Epicentre MasterPure yeast RNA purification kit (Epicentre, Madison, WI) according to manufacturer's instructions. Transcriptomic sequencing using Illumina HiSeq2500 platform and 2 × 150 bp paired-end library was conducted using the services of a commercial provider (Novogene Corporation, Beijing, China) or at the Oklahoma State University Genomics and Proteomics Center. The RNA-seq data were quality trimmed and *de novo* assembled with Trinity (v2.6.6) using default parameters. Redundant transcripts were clustered using CD-HIT [35] with identity parameter of 95% (–c 0.95), and subsequently used for peptide and coding sequence prediction using the TransDecoder (v5.0.2) (https://github.com/TransDecoder/TransDecoder) with a minimum peptide length of 100 amino acids. BUSCO [36] was used to assess transcriptome completeness using the fungi_odb10 dataset modified to remove 155 mitochondrial protein families as previously suggested [30]. The dataset of 52 transcriptomes was used for phylogenomic analysis as described in [37]. In addition, five

Chytridiomycota Genomes (*Chytriomyces* sp. strain MP 71, *Entophlyctis helioformis* JEL805, *Gaertneriomyces semiglobifer* Barr 43, *Gonapodya prolifera* JEL478, and *Rhizoclosmatium globosum* JEL800) were included to provide calibration points. The same phylogenomic dataset (670 protein-coding genes) produced for [37] was used as the original input. Gap regions were removed using trimAl v1.4 [38]. Alignment files that contained no missing taxa and were longer than 150 nucleotide sites were selected for subsequent analyses. By employing a greedy search in PartitionFinder v2.1.1 [39], the 88 selected alignments were grouped into 15 partitions with independent substitution models. All partition files and respective models were loaded in BEAUti v1.10.4 [40] with calibration priors specified as previously described [28] ((i) a direct fossil record of Chytridiomycota from the Rhynie Chert (407 Mya) & (ii) the emergence time of Chytridiomycota (573 to 770 Mya as 95% HPD)) for Bayesian inference and divergence time estimation implemented in BEAST v1.10.4. The Birth-Death incomplete sampling tree model was employed for interspecies relationship analyses. Unlinked strict clock models were used for each partition independently. Three independent runs were performed for 50 million generations and Tracer v1.7.1 [41] was used to confirm that sufficient effective sample size (ESS>200) was reached after the default burn-in (10%). The maximum clade credibility (MCC) tree was compiled using TreeAnnotator v1.10.4 [40].

**Shotgun metagenomic sequencing.** DNA from a subset of samples (n=9) from a cow (n=1), horse (n=1), goats (n=1), sheep (n=1), white-tail deer (n=1), bison (n=1), buffalo (n=1), camel (n=1), and elephant (n=1) was used as a template for metagenomic sequencing on a NextSeq 2K P2 2 × 300-bp paired-end technology with standard library prep using IDT XGen library kit. Sequencing was conducted at the University of Oklahoma Clinical Genomics Facility.

**Metagenomic reads processing.** FastQC was used to assess the quality of metagenomic reads and Trimmomatic v.0.36 [42] was used to trim reads to remove adapters and remove low-quality reads with a sliding window size of 4 and a sliding window minimum quality of 15. High-quality reads were classified at the phylum level using Kaiju v1.7.3 [43] and a reference database comprised of protein sequences from NCBI nr covering Bacteria, Archaea, Viruses, Fungi, and microbial eukaryotes. Reads were also classified using GOTTCHA2 (https://github.com/poeli/GOTTCHA2 ) against fungal nucleotide unique signature sequences built from NCBI RefSeq Release 90. High-quality reads were assembled into contigs using IDBA-UD [44] and a minimum contig length of 2000 bp. For binning eukaryotic genomes from the metagenomic assemblies, we used EukRep [45] to identify and output contigs of potential eukaryotic origins. These potential eukaryotic contigs were then binned using CONCOCT v.1.1 [46] with a minimum contig length of 2500 bp, and a Kmer length of 4. The obtained bins were then filtered to remove all bins <1M bp as previously suggested. For all remaining bins, a prokaryotic classifier (GTDB-Tk) [47] was used to identify and classify falsely identified prokaryotic bins. All steps for read processing and assembly (with the exception of EukRep) were run through Kbase [48, 49, 50]. The outline of the pipeline used is shown in Figure S13.

**Quantitative PCR.** We quantified and compared total AGF to total bacterial load in a subset of the samples comprised of ten cattle, ten goats, ten sheep, and ten horses using quantitative PCR. This was done to further confirm the extremely low relative abundance of AGF DNA when compared to bacterial DNA in the herbivorous feces. The 25-µl PCR reaction volume contained 1 µl of extracted DNA, 0.3 µM of primers AGF-LSU-EnvS primer pair (AGF-LSU-EnvS For: 5'-GCGTTTRRCACCASTGTTGTT-3' and AGF-LSU-EnvS Rev: 5'-GTCAACATCCTAAGYGTAGGTA-3') [7] targeting a ~370 bp region of the LSU rRNA gene

425 (corresponding to the D2 domain), and SYBR GreenER™ qPCR SuperMix for iCycler™
426 (ThermoFisher, Waltham, Massachusetts). Reactions were run on a MyiQ thermocycler (Bio-
427 Rad Laboratories, Hercules, CA). The reactions were heated at 95°C for 8.5 min, followed by 40
428 cycles, with one cycle consisting of 15 sec at 95°C and 1 min at 55°C. Reactions were run in
429 parallel with a pCR 4-TOPO or pCR-XL-2-TOPO plasmid (ThermoFisher, Waltham,
430 Massachusetts) containing an insert spanning ITS1-5.8S rRNA-ITS2-D1/D2 region of 28S rRNA
431 from a pure culture strain as a positive control, as well as to generate a standard curve. The
432 efficiency of the amplification of standards ($E$) was calculated from the slope of the standard
433 curve using the equation $E = (10^{-1/\text{slope}}) - 1$ and was found to be 0.89. Given the variation in the
434 number of rRNA loci in AGF genomes, we opted to quantify AGF in fecal samples as the number of
435 LSU rRNA copies/ g sample, where the number of copies was calculated from the standard curve
436 then converted to copies/g feces based on the volume included in the reaction and the original
437 weight of the fecal samples. Bacterial load was also quantified in the same 40 samples using the
438 515F and 806R prokaryotic-specific primer pair [51] amplifying 16S rRNA V4 hypervariable
439 region. The number of copies of 16S rRNA in each was calculated from standard curves
440 constructed using pCR 4-TOPO plasmid (ThermoFisher, Waltham, Massachusetts) containing an
441 insert spanning the full 16S rRNA from a pure culture strain, then converted to copies/g feces
442 based on the volume included in the reaction and the original weight of the fecal samples.
443

## II. Supplementary figures.

**Figure S1: Rarefaction curve** Rarefaction curves showing the increase in the number of genera observed as the number of sequences increases per sample. Rarefaction data were calculated and plotted in R using rarecurve in vegan.

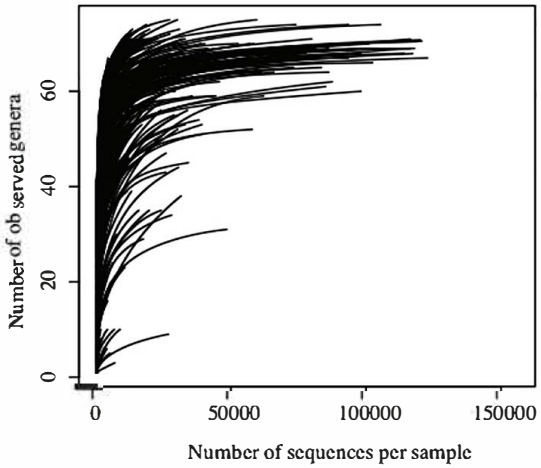
Number of observed genera
0
20
40
60
0
50000
100000
150000
Number of sequences per sample

**Figure S2: Occurrence and relative abundance distribution of all AGF genera encountered in this study.** (A) Number of samples (out of 661) in which each AGF genus was identified. Genera are shown in descending order of their average percentage abundance across samples. (B) Box and whisker plot showing the distribution of the percentage abundance of the 84 genera. Genera are shown in the same order as in (A).

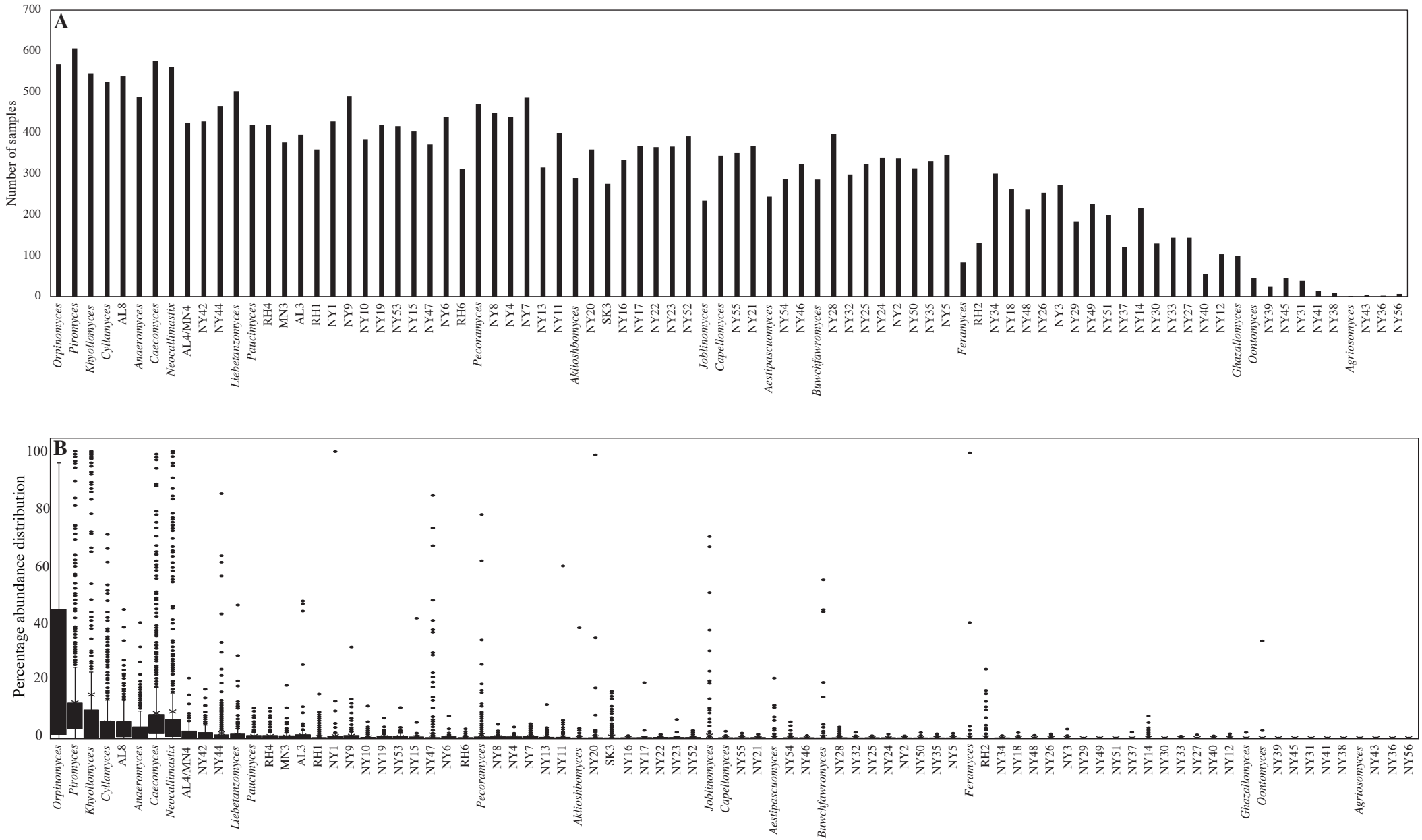
A
Number of samples
0
100
200
300
400
500
600
700
Orpinomyces
Piromyces
Khyollomyces
Cyllamyces
AL8
Anaeromyces
Caecomyces
Neocallimastix
AL4/MN4
NY42
NY44
Liebetanzomyces
Paucimyces
RH4
MN3
AL3
RH1
NY1
NY9
NY10
NY19
NY53
NY15
NY47
NY6
RH6
Pecoramyces
NY8
NY4
NY7
NY13
NY11
Aklioshbomyces
NY20
SK3
NY16
NY17
NY22
NY23
NY52
Joblinomyces
Capellomyces
NY55
NY21
Aestipascuomyces
NY54
NY46
Buwchfawromyces
NY28
NY32
NY25
NY24
NY2
NY50
NY35
NY5
Feramyces
RH2
NY34
NY18
NY48
NY26
NY3
NY29
NY49
NY51
NY37
NY14
NY30
NY33
NY27
NY40
NY12
Ghazallomyces
Oontomyces
NY39
NY45
NY31
NY41
NY38
Agriosomyces
NY43
NY36
NY56


B
Percentage abundance distribution
0
20
40
60
80
100
Orpinomyces
Piromyces
Khyollomyces
Cyllamyces
AL8
Anaeromyces
Caecomyces
Neocallimastix
AL4/MN4
NY42
NY44
Liebetanzomyces
Paucimyces
RH4
MN3
AL3
RH1
NY1
NY9
NY10
NY19
NY53
NY15
NY47
NY6
RH6
Pecoramyces
NY8
NY4
NY7
NY13
NY11
Aklioshbomyces
NY20
SK3
NY16
NY17
NY22
NY23
NY52
Joblinomyces
Capellomyces
NY55
NY21
Aestipascuomyces
NY54
NY46
Buwchfawromyces
NY28
NY32
NY25
NY24
NY2
NY50
NY35
NY5
Feramyces
RH2
NY34
NY18
NY48
NY26
NY3
NY29
NY49
NY51
NY37
NY14
NY30
NY33
NY27
NY40
NY12
Ghazallomyces
Oontomyces
NY39
NY45
NY31
NY41
NY38
Agriosomyces
NY43
NY36
NY56

**Figure S3: Abundance-occurrence plots**. Relationship between occurrence (number of samples) and average relative abundance of each of the 84 genera encountered in this study. The number of samples in which the genera were identified is shown on the X-axis. Average percentage abundance across samples is plotted on the Y axis in a logarithmic scale to show genera present below 1% abundance. Occurrence and relative abundance of different genera were largely correlated ($R^2$=0.71), with the few highlighted exceptions (*Joblinomyces*, *Feramyces*, *Onotomyces*, and RH2).

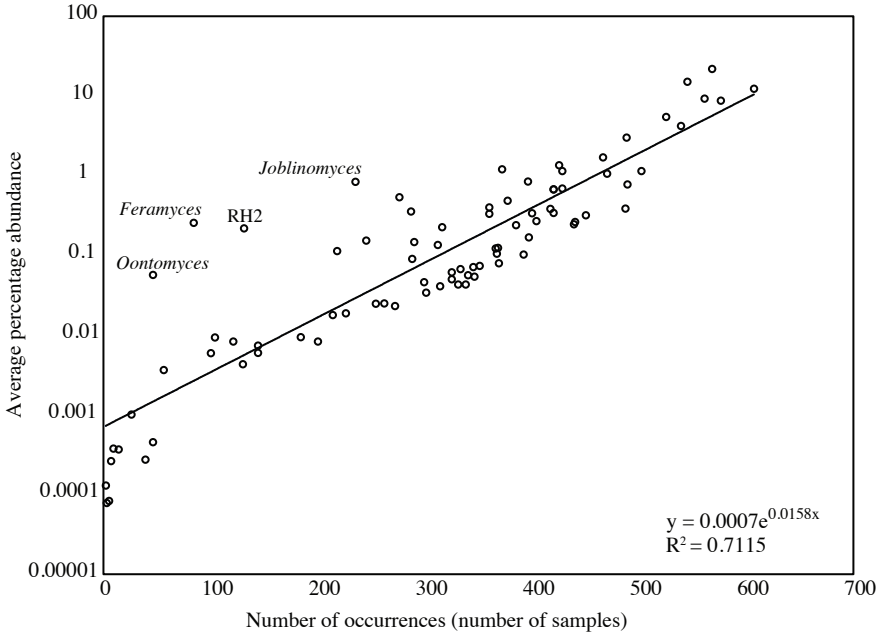
100
10
1
0.1
0.01
0.001
0.0001
0.00001
Average percentage abundance
Joblinomyces
Feramyces
RH2
Oontomyces
y = 0.0007e^0.0158x
R² = 0.7115
0
100
200
300
400
500
600
700
Number of occurrences (number of samples)

**Figure S4: Comparison of community structure patterns between Illumina- and SMRT PacBio-generated datasets.** Comparative analysis of the community structure and composition in 61 samples (60 cows and 1 bison) that were amplified using the D2-targeting primers and sequenced with Illumina sequencing technology, as well as using a different set of primers targeting the whole D1/D2 region and sequenced using the PacBio sequencing technology. (A) AGF community composition in the 61 samples sequenced using Illumina (left stacked bar) and SMRT (right stacked bar) sequencing technologies showing the overall similarity in community composition. (B-D) Community structure in the 61 samples sequenced with the two sequencing technologies. (B) Canonical correspondence analysis (CCA) of the AGF community in the 122 samples (61 samples x 2 sequencing technologies) showing the similarity in community between Illumina-sequenced (red) and SMRT-sequenced (blue) samples. The community structures of the same sample sequenced with the two sequencing technologies were similar (clustered close to each other on the CCA plot). This is evident from the comparisons of the distribution of Euclidean distances on the CCA plot between all possible pairs of Illumina-sequenced samples (red), all possible pairs of SMRT-sequenced samples (blue), and the 61 pairs of Illumina versus PacBio sequenced samples (grey) (C), where the Euclidean distances between the Illumina-SMRT pairs are smaller. Data for the grey box and whisker plot in (C) (the 61 Illumina-SMRT pairs) is shown in detail in (D). Fifty-two pairs lie within a Euclidean distance of 1 from each other, and only 9 pairs lie within a higher Euclidean distance from each other, attesting to the similarity in community composition between the pairs originating from the same sample.

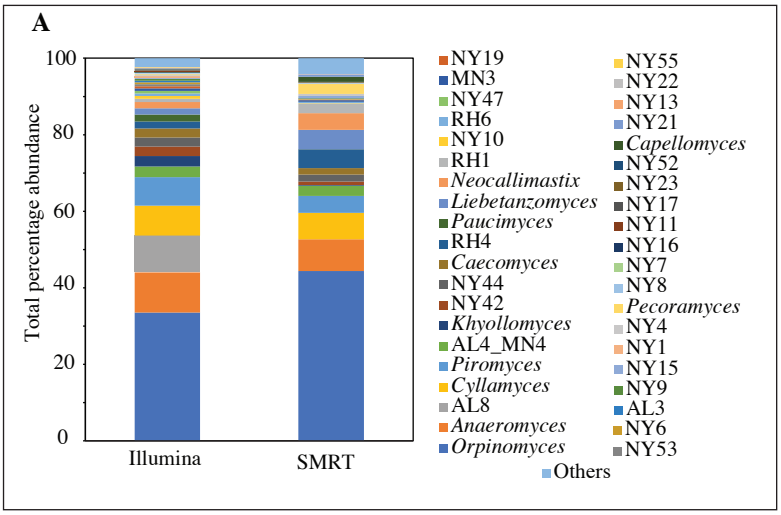
A
Total percentage abundance
100
80
60
40
20
0
Illumina
SMRT
NY19
MN3
NY47
RH6
NY10
RH1
Neocallimastix
Liebetanzomyces
Paucimyces
RH4
Caecomyces
NY44
NY42
Khyollomyces
AL4_MN4
Piromyces
Cyllamyces
AL8
Anaeromyces
Orpinomyces
NY55
NY22
NY13
NY21
Capellomyces
NY52
NY23
NY17
NY11
NY16
NY7
NY8
Pecoramyces
NY4
NY1
NY15
NY9
AL3
NY6
NY53
Others

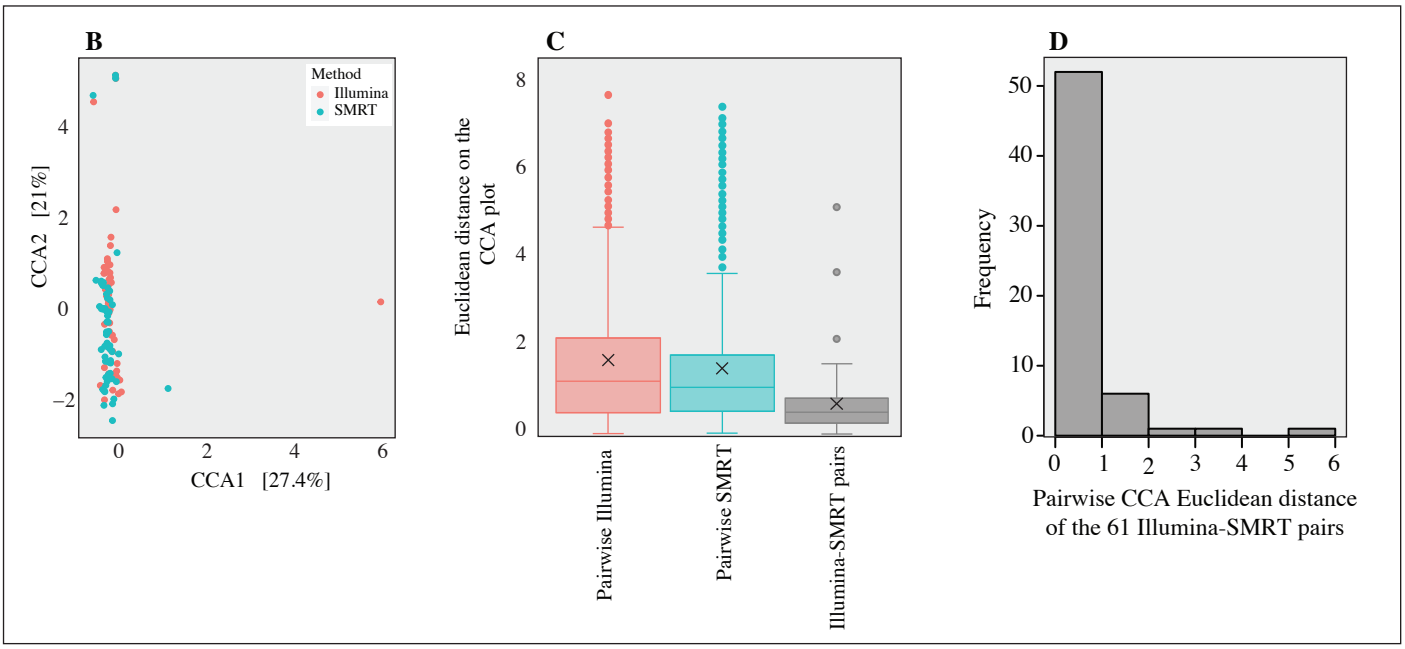
B
Method
Illumina
SMRT
CCA2 [21%]
CCA1 [27.4%]
C
Euclidean distance on the CCA plot
Pairwise Illumina
Pairwise SMRT
Illumina-SMRT pairs
D
Frequency
Pairwise CCA Euclidean distance of the 61 Illumina-SMRT pairs

**Figure S5. Confirmation of the unique position of novel AGF genera (identified using D2 LSU amplicons and Illumina sequencing) using longer D1/D2 LSU amplicons and PacBio sequencing.** Maximum likelihood phylogenetic tree constructed using the alignment of the D1/D2 region from representatives of all cultured (blue) and uncultured (orange) genera, the D1/D2 region from representatives of the 49 novel genera (green) identified by PacBio sequencing in this study and the D2 region from representatives of the 7 novel genera that were not identified in the PacBio dataset. Clades of genera are color-coded by family as shown in the labels around the tree (for the newly proposed families *Neocallimastigaceae*, *Caecomycetaceae*, *Piromycetaceae*, and *Anaeromycetaceae*). Putative novel families encompassing multiple of the novel genera identified here, as well as genera previously unaffiliated with the above four families are shown in red labels around the tree. These include novel families affiliated with the genus *Khoyollomyces*, the genus *Joblinomyces*, the genera *Buwchfawromyces* and *Tahromyces*, the genus *Aklioshbomyces*, and the genus *Paucimyces*. Bootstrap support is shown as black dots for nodes with >70% support.

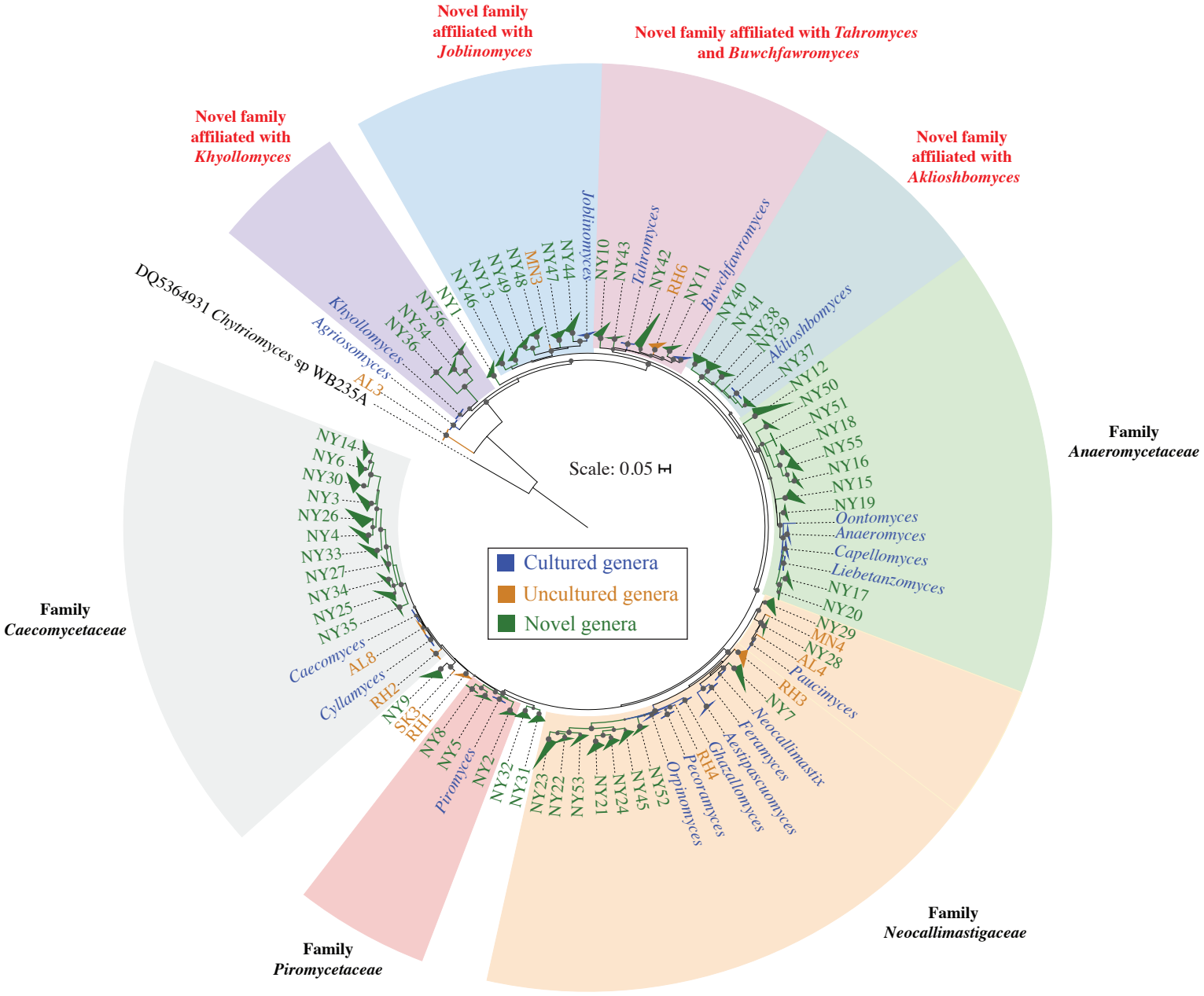
Novel family affiliated with Joblinomyces
Novel family affiliated with Tahromyces and Buwchfawromyces
Novel family affiliated with Khyollomyces
Novel family affiliated with Aklioshbomyces
DQ5364931 Chytriomyces sp WB235A
Scale: 0.05
Cultured genera
Uncultured genera
Novel genera
Family Anaeromycetaceae
Family Caecomycetaceae
Family Piromycetaceae
Family Neocallimastigaceae
Joblinomyces
Tahromyces
Buwchfawromyces
Aklioshbomyces
Khyollomyces
Agriosomyces
Oontomyces
Anaeromyces
Capellomyces
Liebetanzomyces
Paucimyces
Caecomyces
Cyllamyces
Piromyces
Neocallimastix
Feramyces
Aestipascuomyces
Ghazallomyces
Pecoramyces
Orpinomyces

**Figure S6.** Comparison of the topologies of the two maximum likelihood phylogenetic trees constructed using the alignment of the D2 region obtained via Illumina sequencing (left) versus the D1/D2 region obtained using PacBio sequencing (right). Both trees show representatives of all cultured, uncultured, and the 49 novel genera that were identified in both the Illumina and the PacBio datasets. The 7 novel genera that were not identified in the PacBio dataset are shown in red text (only in the Illumina tree). Families and putative families are color coded using the same color code in Figure 2a and Figure S5. The majority of genera (79 out of 87 total) had a similar topology in both trees (i.e., belonged to the same family or putative family). The 8 genera with discrepant topology in the two trees are shown in boldface. The trees were rooted using *Chytriomyces* sp. WB235A as an outgroup (not shown)

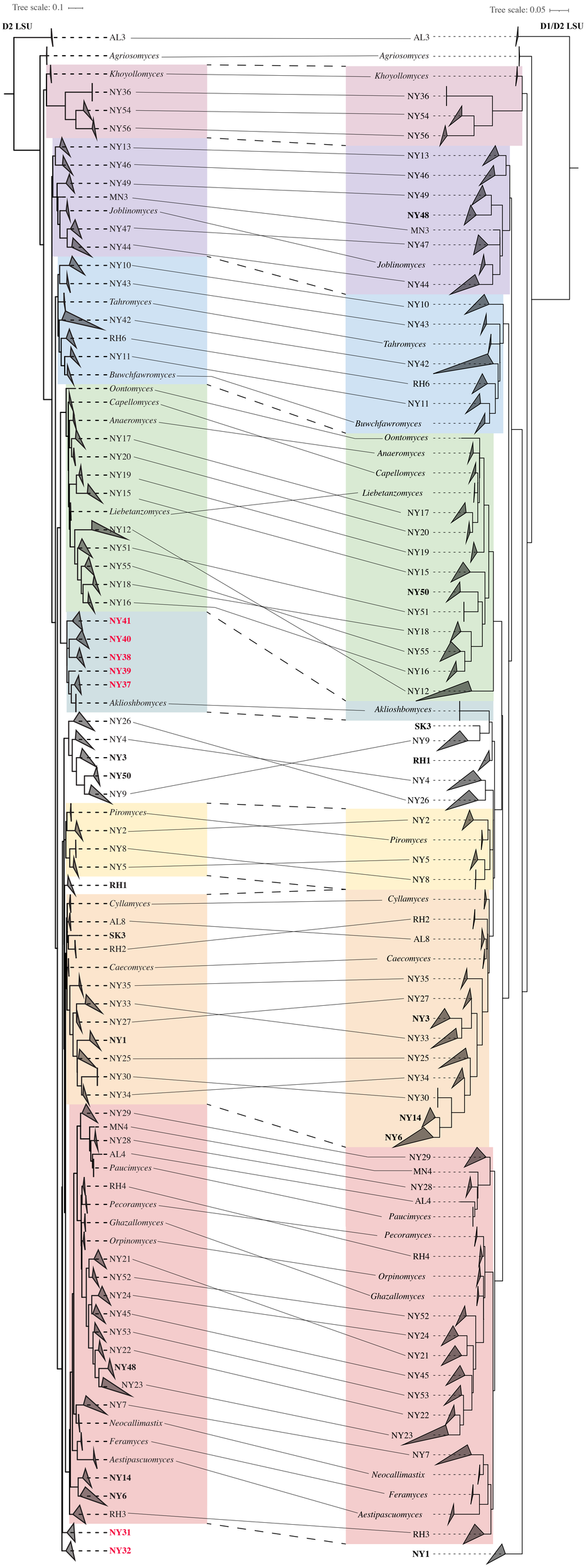
Tree scale: 0.1
D2 LSU
AL3
Agriosomyces
Khoyollomyces
NY36
NY54
NY56
NY13
NY46
NY49
MN3
Joblinomyces
NY47
NY44
NY10
NY43
Tahromyces
NY42
RH6
NY11
Buwchfawromyces
Oontomyces
Capellomyces
Anaeromyces
NY17
NY20
NY19
NY15
Liebetanzomyces
NY12
NY51
NY55
NY18
NY16
NY41
NY40
NY38
NY39
NY37
Aklioshbomyces
NY26
NY4
NY3
NY50
NY9
Piromyces
NY2
NY8
NY5
RH1
Cyllamyces
AL8
SK3
RH2
Caecomyces
NY35
NY33
NY27
NY1
NY25
NY30
NY34
NY29
MN4
NY28
AL4
Paucimyces
RH4
Pecoramyces
Ghazallomyces
Orpinomyces
NY21
NY52
NY24
NY45
NY53
NY22
NY48
NY23
NY7
Neocallimastix
Feramyces
Aestipascuomyces
NY14
NY6
RH3
NY31
NY32
Tree scale: 0.05
D1/D2 LSU
AL3
Agriosomyces
Khoyollomyces
NY36
NY54
NY56
NY13
NY46
NY49
NY48
MN3
NY47
Joblinomyces
NY44
NY10
NY43
Tahromyces
NY42
RH6
NY11
Buwchfawromyces
Oontomyces
Anaeromyces
Capellomyces
Liebetanzomyces
NY17
NY20
NY19
NY15
NY50
NY51
NY18
NY55
NY16
NY12
Aklioshbomyces
SK3
NY9
RH1
NY4
NY26
NY2
Piromyces
NY5
NY8
Cyllamyces
RH2
AL8
Caecomyces
NY35
NY27
NY3
NY33
NY25
NY34
NY30
NY14
NY6
NY29
MN4
NY28
AL4
Paucimyces
Pecoramyces
RH4
Orpinomyces
Ghazallomyces
NY52
NY24
NY21
NY45
NY53
NY22
NY23
NY7
Neocallimastix
Feramyces
Aestipascuomyces
RH3
NY1

**Fig. S7. Patterns of AGF alpha diversity.** Samples with at least 1000 sequences were included (n=421); and the analysis was repeated with and without randomly subsampling 1000 sequences from each sample. Alpha diversity patterns were assessed using four different indices (observed number of genera, Shannon, Simpson, and Inverse Simpson) and the two sampling strategies. (A) Box and whisker plots showing the distribution of 4 alpha diversity measures for different animal species (top row), animal families (middle row), and animal gut types (bottom row). (B) Results of ANOVA showing the significant effect of the host species, animal family, and animal gut type, but not domestication status, on alpha diversity measures regardless of the index used or the subsampling approach ($p<0.0002$). (C) Tukey test results for pairwise animal species, animal family, and animal gut type comparisons (8 comparisons each; 2 subsampling approaches x 4 diversity indices). Specifically, hindgut animals harbored a significantly less diverse community compared to foregut ruminants (in all 8 comparisons; p-value <0.00001). Accordingly, members of the hindgut family Equidae harbored a less diverse community when compared to the foregut ruminant families Cervidae and Bovidae (in 6/8 comparisons; p-value <0.002, and in 6/8 comparisons; p-value <0.00004, respectively); and horse communities were significantly less diverse than these of deer (in 6/8 comparisons; p-value <0.04), cattle (in 6/8 comparisons; p-value <0.00004), goats (in 6/8 comparisons; p-value <0.02), and sheep (in 4/8 comparisons; p-value <0.01). Within foregut ruminants, communities in animals belonging to the families Cervidae and Bovidae were not significantly different (7/8 comparisons; p-value >0.09). As well, on the animal host species level, most comparisons indicated no significant differences in diversity between deer, goat, cattle, and sheep.

**A**

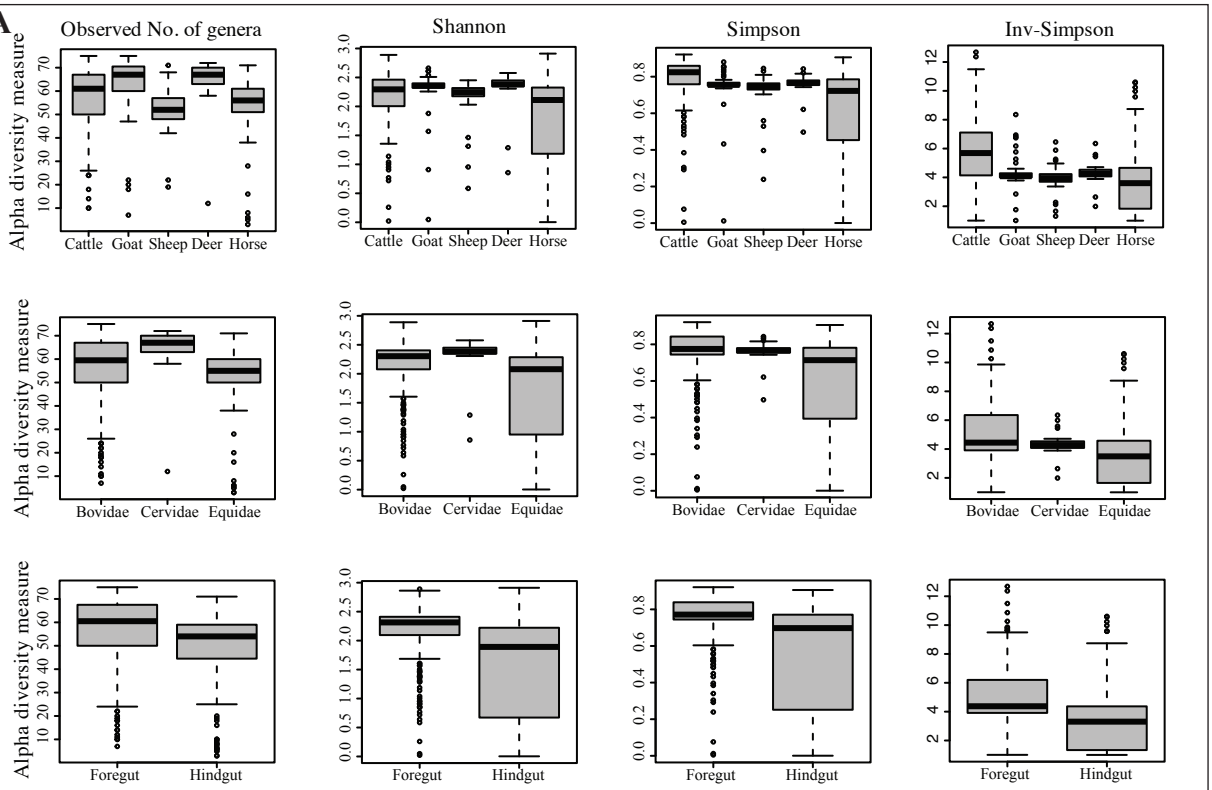


**B**

| Host factor | Observed No. of genera | | Shannon | | Simpson | | Inv-Simpson | |
|---|---|---|---|---|---|---|---|---|
| | With subsampling | Without subsampling | With subsampling | Without subsampling | With subsampling | Without subsampling | With subsampling | Without subsampling |
| Animal species | 1.7E-15 | 1.4E-06 | 8.4E-06 | 0.0001 | 8E-05 | 0.0001 | 9.9E-08 | 4.2E-08 |
| Family | 2E-16 | 2E-16 | 2.2E-15 | 1E-14 | 1.5E-14 | 4.8E-13 | 1.6E-06 | 9E-07 |
| Gut type | 6.5E-10 | 9.2E-12 | 2E-16 | 2E-16 | 2E-16 | 2E-16 | 1.5E-08 | 3.2E-08 |
| Domestication | NS | NS | NS | NS | NS | NS | NS | NS |

**C**

| Host factor | Group1 | Group 2 | With subsampling | | | | Without subsampling | | | |
|---|---|---|---|---|---|---|---|---|---|---|
| | | | Observed No. of genera | Shannon | Simpson | Inv-Simpson | Observed No. of genera | Shannon | Simpson | Inv-Simpson |
| Animal Species | Deer | Cattle | 0.0000002 | 0.99 | 1 | 0.3 | 0.43 | 0.99 | 1 | 0.3 |
| | Goat | Cattle | 0 | 0.95 | 1 | 0.051 | 0.34 | 0.94 | 1 | 0.049 |
| | Goat | Deer | 1 | 1 | 1 | 1 | 1 | 1 | 1 | 1 |
| | Horse | Cattle | 0.99 | 0.00004 | 0 | 0.0000003 | 0.97 | 0.00004 | 0 | 0.0000002 |
| | Horse | Deer | 0.0003 | 0.0009 | 0.015 | 0.99 | 0.04 | 0.0008 | 0.015 | 0.99 |
| | Horse | Goat | 0.000007 | 0.000004 | 0.0001 | 0.99 | 0.015 | 0.000004 | 0.0001 | 0.99 |
| | Sheep | Cattle | 0.00004 | 1 | 0.97 | 0.00002 | 0.92 | 1 | 0.96 | 0.00002 |
| | Sheep | Deer | 0.89 | 0.99 | 1 | 0.99 | 0.03 | 0.99 | 1 | 0.99 |
| | Sheep | Goat | 0.9 | 0.99 | 0.99 | 0.99 | 0.013 | 0.99 | 0.99 | 0.99 |
| | Sheep | Horse | 0.079 | 0.003 | 0.01 | 1 | 1 | 0.005 | 0.001 | 1 |
| Animal Family | Cervidae | Bovidae | 0.0006 | 0.84 | 1 | 0.86 | 0.09 | 0.83 | 1 | 0.86 |
| | Equidae | Bovidae | 0.47 | 0 | 0 | 0.00004 | 0.11 | 0 | 0 | 0.00003 |
| | Equidae | Cervidae | 0.00002 | 0.000008 | 0.0001 | 0.91 | 0.001 | 0.000006 | 0.0001 | 0.90 |
| Gut type | Hindgut | Foregut | 0.00001 | 0 | 0 | 0.0000002 | 0.0000006 | 0 | 0 | 0.0000002 |

**Figure S8.** Ordination plots based on AGF community structure in the 661 samples studied here. (A) RDA plot constructed using the center log-ratio transformed genera abundance data. The % variance explained by the first two axes are displayed on the axes. (B) Non-metric dimensional scaling (NMDS) plots based on the phylogenetic similarity-based (unweighted and weighted Unifrac) indices as shown above each plot. NMDS stress value is shown in the upper corner of each plot. (C) Principal coordinate analysis (PCoA) plot based on the phylogenetic similarity-based index unweighted Unifrac. The % variance explained by the first two axes are displayed on the axes. Samples are color-coded by animal species, while the shape depicts the gut type.

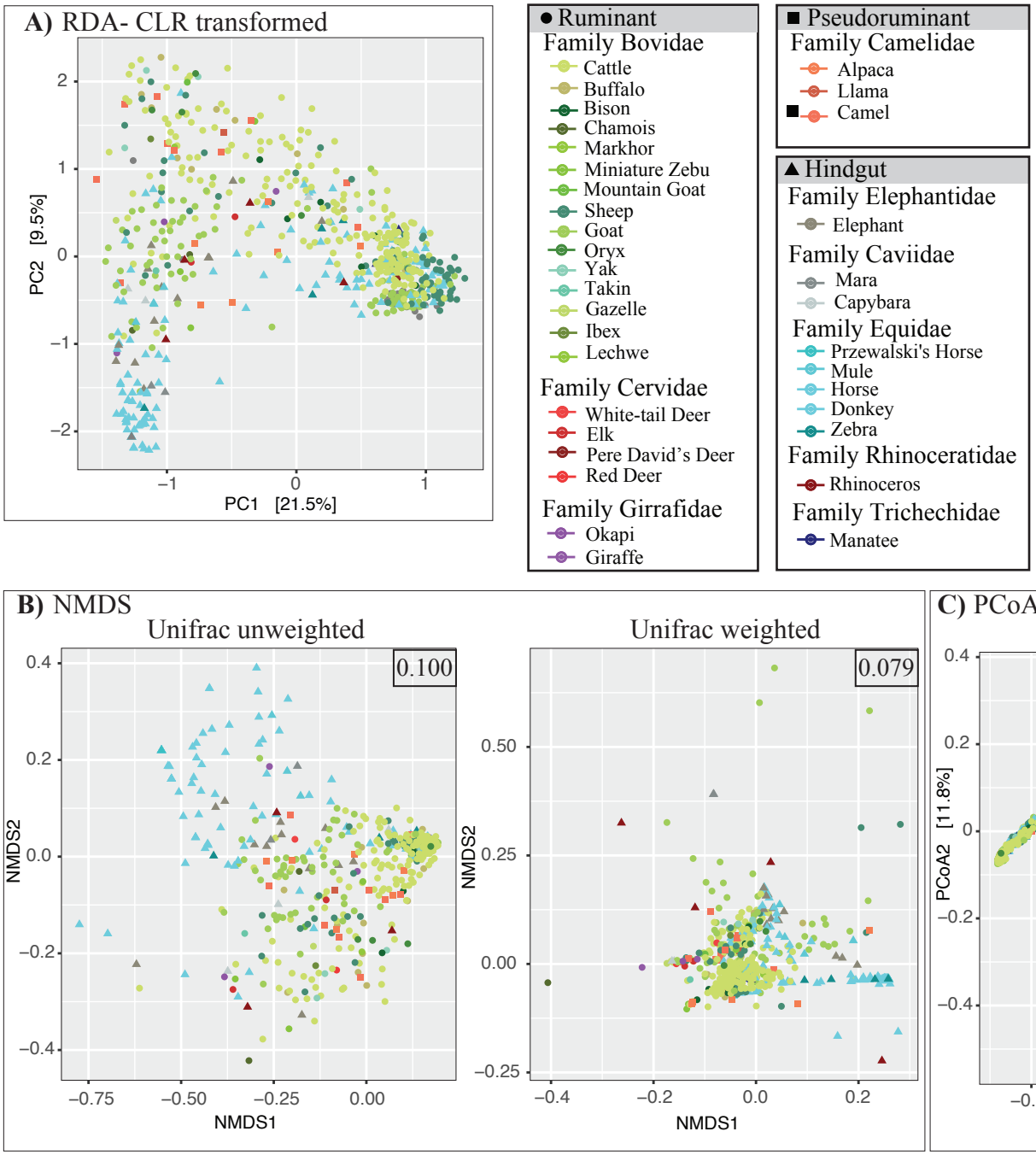
A) RDA- CLR transformed
PC2 [9.5%]
PC1 [21.5%]
Ruminant
Family Bovidae
Cattle
Buffalo
Bison
Chamois
Markhor
Miniature Zebu
Mountain Goat
Sheep
Goat
Oryx
Yak
Takin
Gazelle
Ibex
Lechwe
Family Cervidae
White-tail Deer
Elk
Pere David's Deer
Red Deer
Family Girrafidae
Okapi
Giraffe
Pseudoruminant
Family Camelidae
Alpaca
Llama
Camel
Hindgut
Family Elephantidae
Elephant
Family Caviidae
Mara
Capybara
Family Equidae
Przewalski's Horse
Mule
Horse
Donkey
Zebra
Family Rhinoceratidae
Rhinoceros
Family Trichechidae
Manatee


B) NMDS
Unifrac unweighted
0.100
NMDS2
NMDS1
Unifrac weighted
0.079
NMDS2
NMDS1

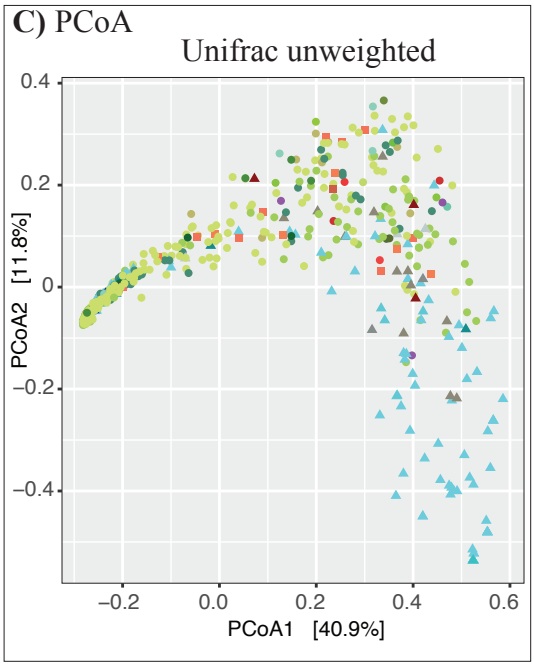
C) PCoA
Unifrac unweighted
PCoA2 [11.8%]
PCoA1 [40.9%]

**Figure S9.** Box and whisker plots of the distribution of PCoA ordination distance of each sample to its group centroid (pink) and all other (non-group, cyan) centroids. The PCoA plots are shown in Fig. 4a. Centroids were calculated using the command betadisper in the vegan package for each animal species (left, only for animals with 4 or more individuals), animal family (middle), and animal gut type (right). Ordination distance between each point and the group centroid was calculated as the Euclidean distance between two points in an ordination plot. In general, samples clustered by the animal species (small variation in Euclidean distance to the animal species centroid), with only a few animals (e.g. horse, donkey, sheep, goat) showing large variation from their respective animal species centroid, usually due to only a few divergent samples. Interestingly, the microbial community structure showed a higher level of "variability" in hindgut animals when compared to foregut. Samples from animals belonging to the foregut families Bovidae, Cervidae, Giraffidae, and Camelidae clustered close to their respective animal family centroid. However, large variation was observed for the hindgut families Equidae, and Caviidae. This was also observed when comparing samples to their respective gut type centroid, where samples from foregut animals clustered close to their gut type centroid, while samples from hindgut animals showed large variation in their distance from the hindgut centroid. (B) Quantitative assessment of host factors affecting community structure via multivariate regression methods (multiple regression of matrices (MRM), Mantel tests for matrices correlations, and Procrustes rotation). Methods compared the AGF community dissimilarity matrix (Unifrac weighted (W), Unifrac unweighted (UW), Bray-Curtis, and Jaccard), to a matrix of each of the host factors tested (animal species, animal family, animal gut type, and domestication status). For the MRM analysis, results of the whole model (without partitioning variances into different host factors) are shown on top. The model was found to be significant regardless of the index used. For each of the three methods, the significance of correlation (depicted as the test p-value),

and the degree the host factor is affecting community structure (depicted by the $R^2$ regression coefficients of the MRM analysis, the Spearman correlation coefficients of the Mantel test, and the symmetric orthogonal Procrustes statistic of the Procrustes analysis) are shown. Significant p-values (<0.05) are shown in red text. Results of matrices correlation (12 total correlations; 3 methods x 4 dissimilarity indices) using each of the three methods, and regardless of the index used, confirmed the importance of animal host species, family, and gut type in explaining the AGF community structure. Animal host species and family were both found to be significant in all 12 correlations (p-value=0.001 for animal species, and <0.025 for animal family), while the animal gut type was found to be significant in 10 out of the 12 correlations (p-value <0.025). Further, comparing the correlation coefficients produced by each of the methods showed that the animal species explains more of the community structure (as evident by the higher $R^2$ regression coefficients of the MRM analysis, the higher Spearman correlation coefficients of the Mantel test, and the higher symmetric orthogonal Procrustes statistic of the Procrustes analysis) than the animal family or the gut type. This was true for 10 out of the 12 correlations. On the other hand, domestication status was only found significant in 3 out of the 12 total correlations, albeit with very low correlation coefficients.

**A**

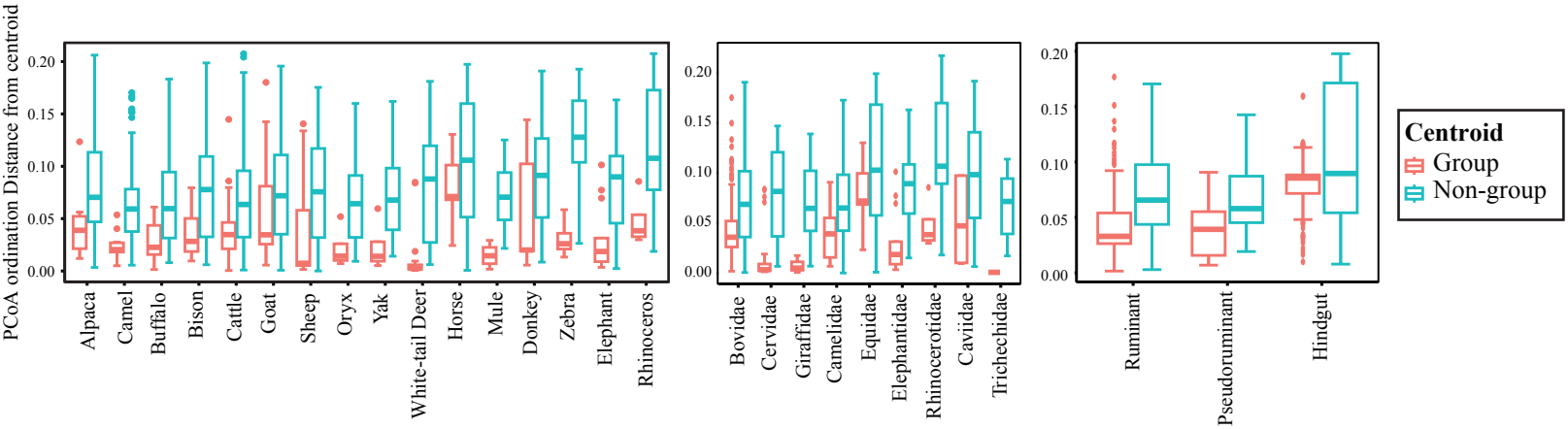


**B**

| Test | Factors | Statistic | Beta diversity index | | | |
|---|---|---|---|---|---|---|
| | | | Unifrac (W) | Unifrac (UW) | Bray-Curtis | Jaccard |
| MRM | Whole model | $R^2$ | 0.147 | 0.050 | 0.041 | 0.039 |
| | | p-value | **0.001** | **0.001** | **0.001** | **0.001** |
| | | F | 9431.8 | 2869.4 | 2315.1 | 2206.3 |
| | | F.p-value | **0.001** | **0.001** | **0.001** | **0.001** |
| | Animal species | p-value | **0.001** | **0.001** | **0.001** | **0.001** |
| | Host family | | **0.024** | **0.015** | **0.001** | **0.001** |
| | Gut Type | | **0.001** | **0.023** | 0.993 | 0.952 |
| | Domestication | | 0.845 | 0.804 | 0.792 | 0.629 |
| | Animal species | Coefficients | 0.342 | 0.178 | 0.199 | 0.252 |
| | Host family | | 0.306 | 0.160 | 0.273 | 0.159 |
| | Gut Type | | 0.120 | 0.052 | 0.000 | -0.001 |
| | Domestication | | -0.001 | 0.004 | 0.002 | 0.003 |
| Mantel | Animal species | p-value | **0.001** | **0.001** | **0.001** | **0.001** |
| | Host family | | **0.001** | **0.001** | **0.001** | **0.001** |
| | Gut Type | | **0.001** | **0.001** | **0.001** | **0.001** |
| | Domestication | | **0.036** | 0.868 | 0.285 | 0.246 |
| | Animal species | Coefficients | 0.377 | 0.217 | 0.182 | 0.175 |
| | Host family | | 0.329 | 0.173 | 0.120 | 0.113 |
| | Gut Type | | 0.371 | 0.208 | 0.156 | 0.148 |
| | Domestication | | 0.051 | 0.027 | 0.019 | 0.020 |
| Procrustes | Animal species | p-value | **0.001** | **0.001** | **0.001** | **0.001** |
| | Host family | | **0.001** | **0.001** | **0.001** | **0.001** |
| | Gut Type | | **0.001** | **0.001** | **0.001** | **0.001** |
| | Domestication | | 0.082 | 0.216 | **0.033** | **0.013** |
| | Animal species | Correlation | 0.507 | 0.305 | 0.279 | 0.272 |
| | Host family | in a | 0.448 | 0.252 | 0.208 | 0.203 |
| | Gut Type | symmetric | 0.491 | 0.491 | 0.219 | 0.210 |
| | Domestication | Procrustes | 0.061 | 0.048 | 0.065 | 0.075 |
| | Animal species | Procrustes | 0.743 | 0.743 | 0.922 | 0.926 |
| | Host family | Sum of | 0.799 | 0.937 | 0.957 | 0.959 |
| | Gut Type | Squares | 0.759 | 0.911 | 0.952 | 0.956 |
| | Domestication | | 0.996 | 0.998 | 0.996 | 0.994 |

**Figure S10: Fungal genera-animal host preferences.** Double principal coordinate analysis (DPCoA) biplot constructed using the genera with abundance in the top 25% of each sample and that were encountered in at least 50% of the samples (n=28 genera). DPCoA uses both abundance and phylogenetic information about the samples, allowing both the samples and the taxa to be plotted on the same coordinate space, and thus the ordination distance between samples or their centroids and AGF genera could be compared. AGF genera with ordination distances close to sample centroids are abundant in these samples, and, therefore, contribute more to the community structure. For ease of visualization, individual samples are removed and only the animal species (hexagons, only for animals with 4 or more individuals), animal family (squares), and animal gut type (X) centroids are plotted, with standard deviation data ellipse shown for only the gut type. Centroids and data ellipses were generated using the command betadisper in the vegan package. Animals are color-coded by their respective family as shown in the key and colors follow the same scheme as in Fig 1d. The AGF genera are shown as purple circles. The first two axes explained 69.4% of the variance. There was a clear separation of the hindgut families Equidae (orange square centroid), Rhinocerotidae (green square centroid), from the foregut families Bovidae (pink square centroid), Cervidae (yellow square centroid), and Giraffidae (red square centroid), with the pseudoruminant family Camelidae (purple square centroid) occupying an intermediate position. Of the 28 most abundant genera, 14 fell within the foregut ruminant ellipses, all of which were shared with the overlapping foregut pseudoruminant ellipse. Three additional genera fell within the foregut pseudoruminant ellipse. Only 9 genera fell within the hindgut ellipse outside the foregut ruminant and pseudoruminant ellipses. These genera included the Equidae-specific *Khoyollomyces* and AL3, the Trichechidae-specific *Paucimyces*, and the Rhinocerotidae-specific NY15. The genera *Orpinomyces*, and NY53 fell

outside all ellipses, consistent with their high LIPA values of association with almost all families, hence their intermediary position on the biplot. Several genera, NY42, NY6, NY7, AL4/MN4, *Cyllamyces*, and AL8, fell within the ellipses of all gut types. These genera had moderate LIPA association values with almost all animal genera. The two genera *Piromyces*, and *Caecomyces* also fell within the ellipses of all gut types, but their position is most probably due to their strong association with the family Elephantidae.

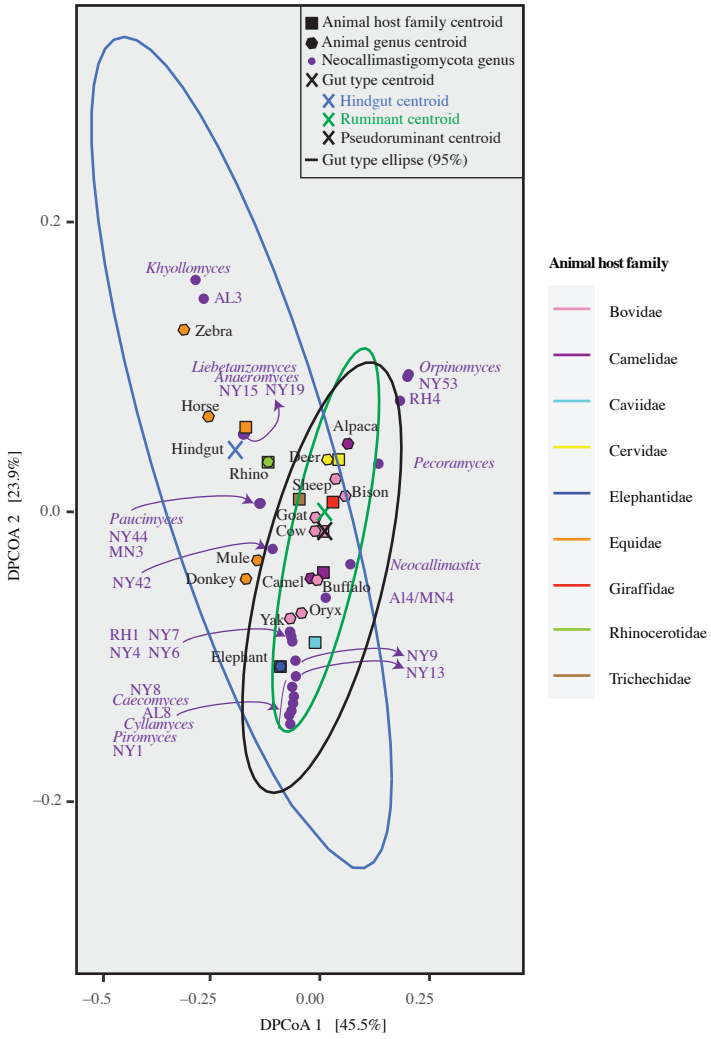
Animal host family centroid
Animal genus centroid
Neocallimastigomycota genus
Gut type centroid
Hindgut centroid
Ruminant centroid
Pseudoruminant centroid
Gut type ellipse (95%)
Khyollomyces
AL3
Zebra
Liebetanzomyces
Anaeromyces
NY15 NY19
Horse
Hindgut
Rhino
Orpinomyces
NY53
RH4
Alpaca
Deer
Pecoramyces
Sheep
Bison
Goat
Cow
Paucimyces
NY44
MN3
NY42
Mule
Donkey
Camel
Buffalo
Neocallimastix
A14/MN4
Oryx
Yak
RH1 NY7
NY4 NY6
Elephant
NY9
NY13
NY8
Caecomyces
AL8
Cyllamyces
Piromyces
NY1
0.2
0.0
−0.2
−0.5
−0.25
0.00
0.25
DPCOA 2 [23.9%]
DPCoA 1 [45.5%]
Animal host family
Bovidae
Camelidae
Caviidae
Cervidae
Elephantidae
Equidae
Giraffidae
Rhinocerotidae
Trichechidae

**Figure S11: Effect of biogeography, age, and sex on AGF community structure in cattle (A, E, I), goats (B, F, J), sheep (C, G, K), and horses (D, H, L).** For testing the effect of biogeography, age, and sex on community structure, we opted to carry out comparisons only on samples belonging to the same animal species in an attempt to control for other host-associated factors that might conflate the results. For these comparisons, only the four most-sampled animal species (cattle, goats, sheep, and horses) were considered. RDA ordination plots constructed using the center log-ratio transformed genera abundance data are shown. The first two PCoA axes are plotted, and the percentage variance explained by each axis is shown for each plot. Samples are color-coded (as shown in the figure color key) by their country of origin (A-D), age (E-H), and sex (I-L). For biogeography effects, samples originated from different geographical locations (Argentina, Austria, Czech Republic, Egypt, Germany, Italy, Nepal, New Zealand, and the USA). For age, animals were classified as young (<1 year), or adult (>1 year), and sex was either male or female. Samples where this information was not available are shown as NA. The first two axes explained 46.1%-55.5% of the variance depending on the animal subset. (M) To test for the significance of the above three factors in describing AGF community structure in each animal genus, PERMANOVA tests were run using the vegan command adonis. The F-statistics p-value was used to assess the significance of AGF community difference between countries, young versus adult animals, and males versus females, and the sum of squares was used to assess the percentage variance explained by the country of origin for each of the four animal species. PERMANOVA tests showed that the country of origin explained 3.9% of variance in cattle AGF communities (F test p-value=0.002), 10.2% of variances in horses AGF communities (F test p-value=0.012), 20.62% of variances in goats AGF communities (F test p-value=0.001), and 33.84% of variances in sheep AGF communities (F test p-value=0.001). On

the other hand, age explained 6-18% of variances, and sex explained 3.1-18% of variances in community structure.

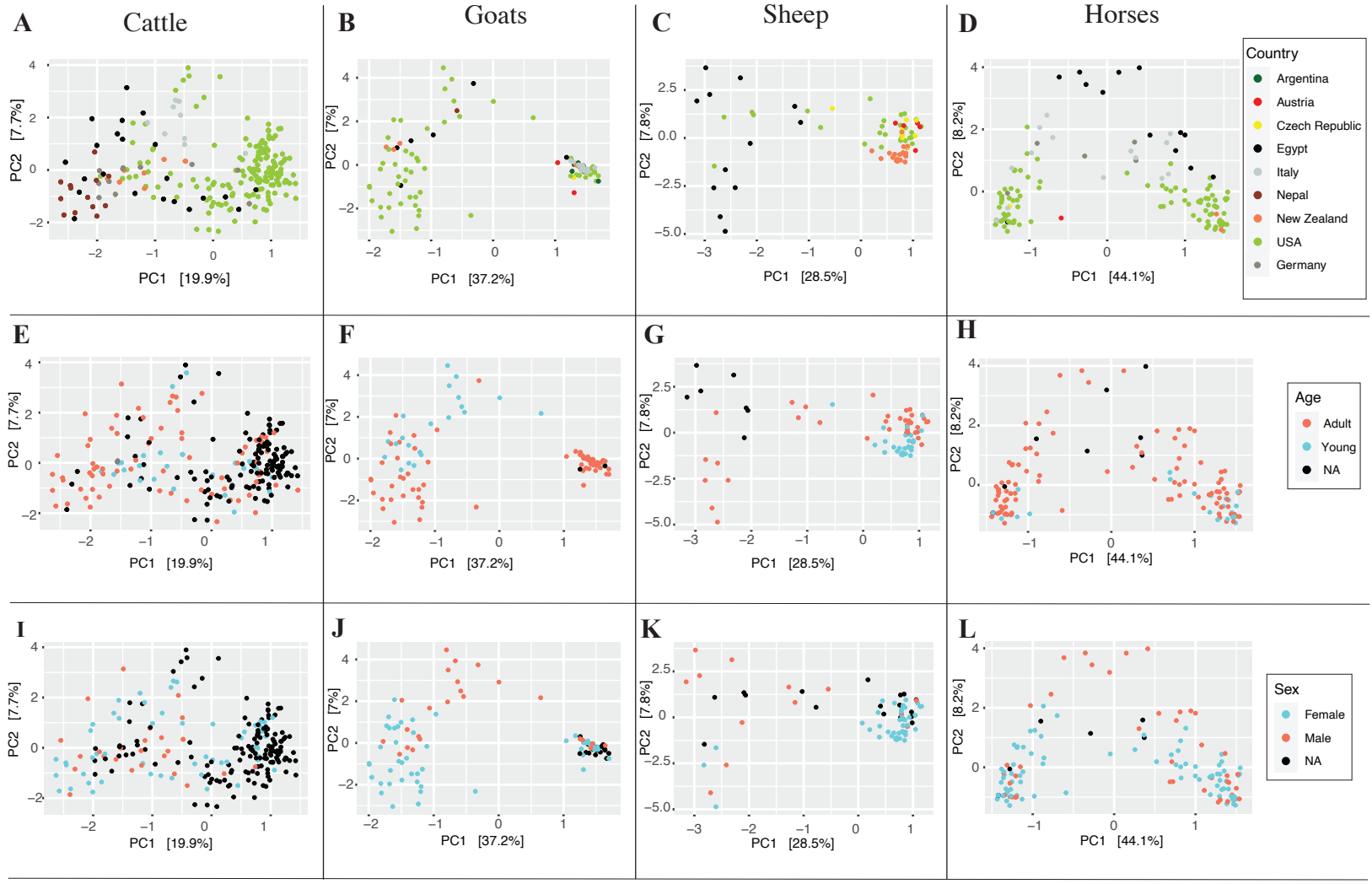


**M**

| Animal species | Factors tested | | | | | |
|---|---|---|---|---|---|---|
| | Biogeography | | Age | | Sex | |
| | p-value | $R^2$ | p-value | $R^2$ | p-value | $R^2$ |
| Cattle | 0.015 | 0.038 | 0.001 | 0.092 | 0.001 | 0.031 |
| Goats | 0.001 | 0.21 | 0.006 | 0.06 | 0.001 | 0.14 |
| Sheep | 0.001 | 0.34 | 0.001 | 0.18 | 0.001 | 0.18 |
| Horses | 0.001 | 0.102 | 0.001 | 0.094 | 0.002 | 0.065 |

**Figure S12.** Results of read classification at the phylum level using Kaiju and GOTTCHA2. Only one sample (from a horse) had reads assigned to Neocallimastigomycota with 0.05% total abundance.

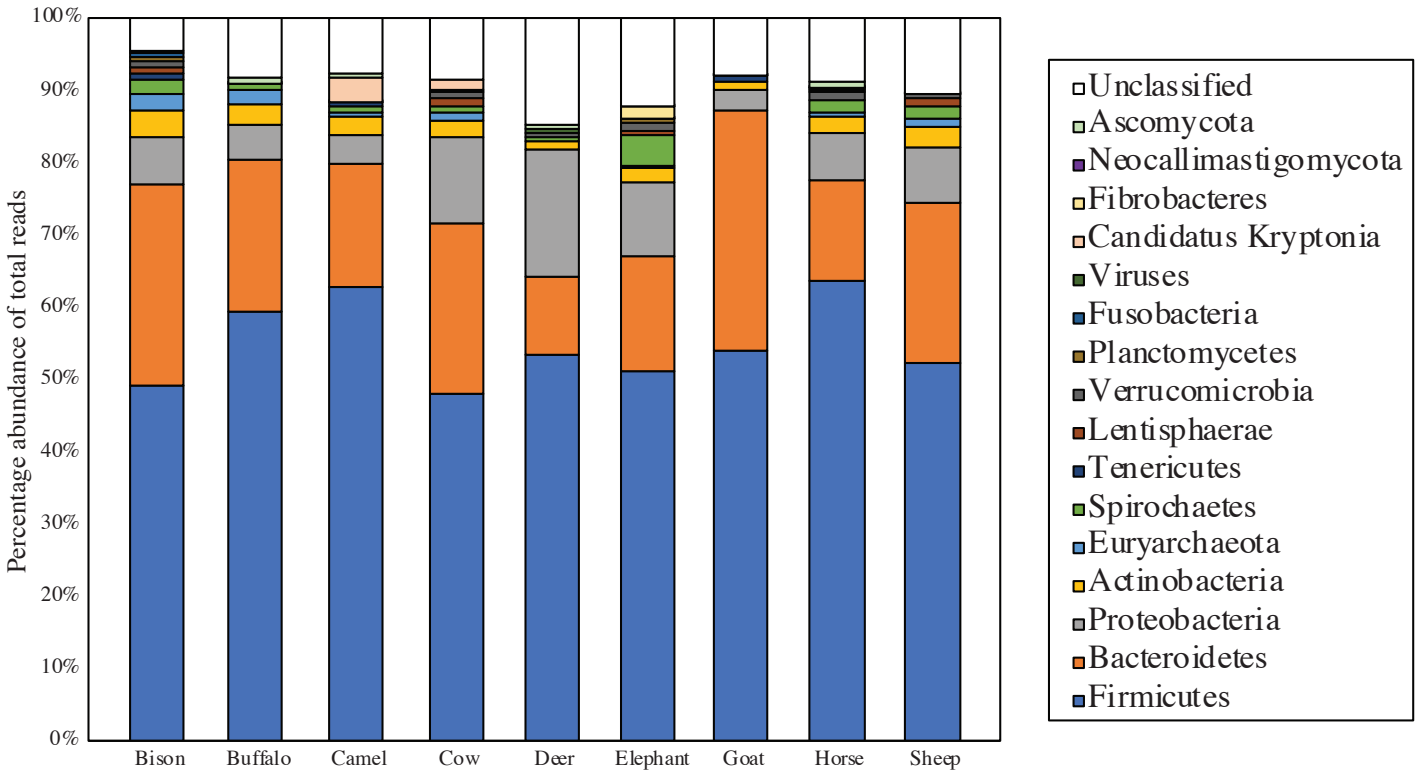
100%
90%
80%
70%
60%
50%
40%
30%
20%
10%
0%
Percentage abundance of total reads
Bison
Buffalo
Camel
Cow
Deer
Elephant
Goat
Horse
Sheep
Unclassified
Ascomycota
Neocallimastigomycota
Fibrobacteres
Candidatus Kryptonia
Viruses
Fusobacteria
Planctomycetes
Verrucomicrobia
Lentisphaerae
Tenericutes
Spirochaetes
Euryarchaeota
Actinobacteria
Proteobacteria
Bacteroidetes
Firmicutes

**Figure S13.** Quantitative PCR (qPCR) analysis to quantify bacterial:AGF rRNA gene copy number in fecal samples. Values are reported as LSU copies/g fecal sample. Boxplots are showing the distribution of the number of AGF and bacterial rRNA copies/g feces from ten individual cattle, goats, sheep, and horses.

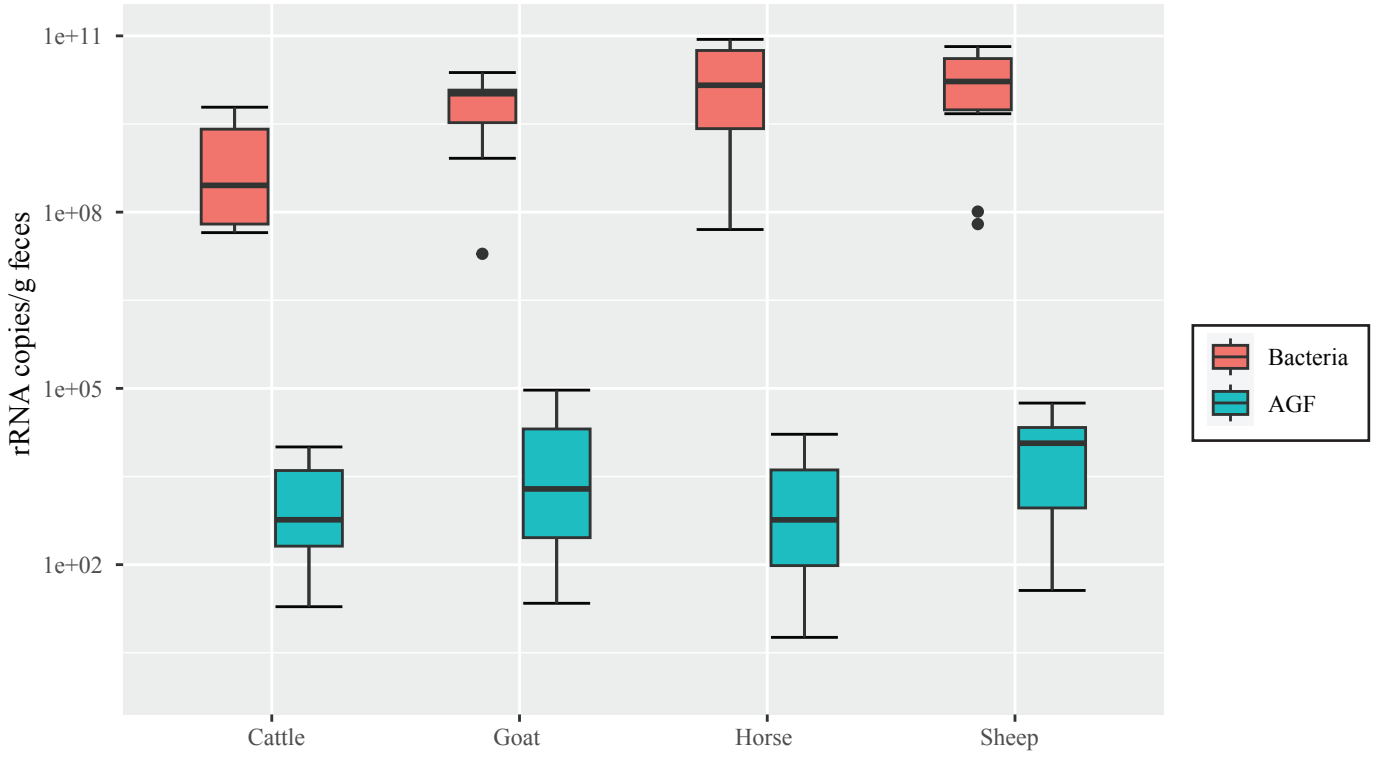
1e+11
1e+08
1e+05
1e+02
rRNA copies/g feces
Cattle
Goat
Horse
Sheep
Bacteria
AGF

**Figure S14: Effect of amplicon length/region on pairwise sequence divergence estimates.** Comparison of all possible pairwise sequence identities of a group of 206 reference sequences, when the whole D1/D2 region was used (as would be obtained by SMRT sequencing using the NL1 forward primer/ GGNL4 reverse primer, X-axis) and when only the D2 region was used (as would be obtained by Illumina sequencing using primers employed here, Y-axis). Sequences were first aligned in MAFFT, and the alignment was used to calculate pairwise distances in MEGA. Aligned long sequences covering the D1/D2 regions were then trimmed in MEGA to remove the D1 region, and this truncated alignment was then used to calculate pairwise distances in MEGA.

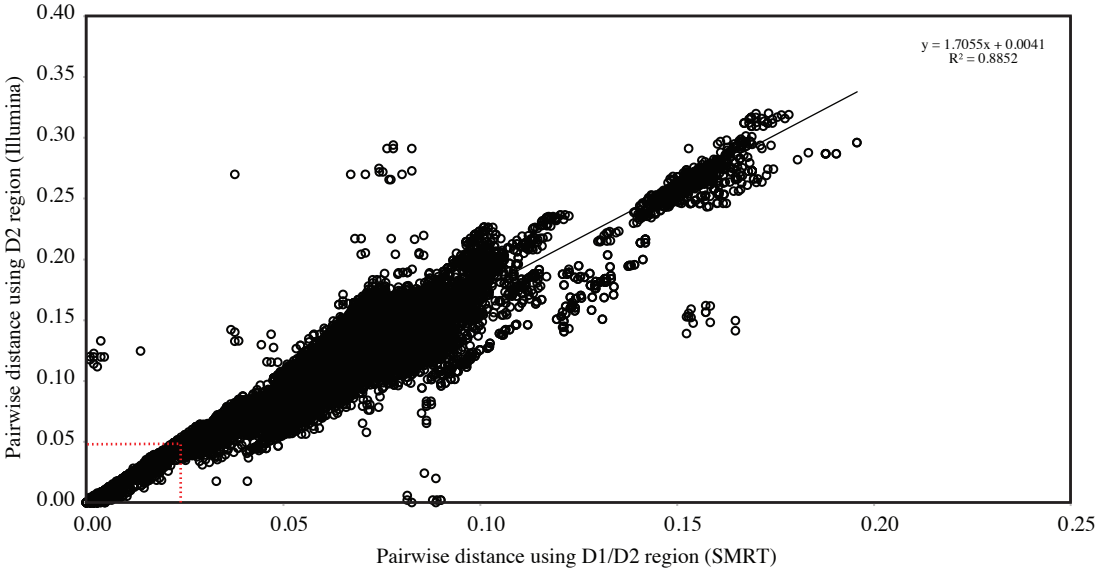
y = 1.7055x + 0.0041
R² = 0.8852
Pairwise distance using D2 region (Illumina)
Pairwise distance using D1/D2 region (SMRT)
0.00
0.05
0.10
0.15
0.20
0.25
0.30
0.35
0.40

**Figure S15.** Outline of the pipeline used to identify, and bin contigs of potential eukaryotic origin.

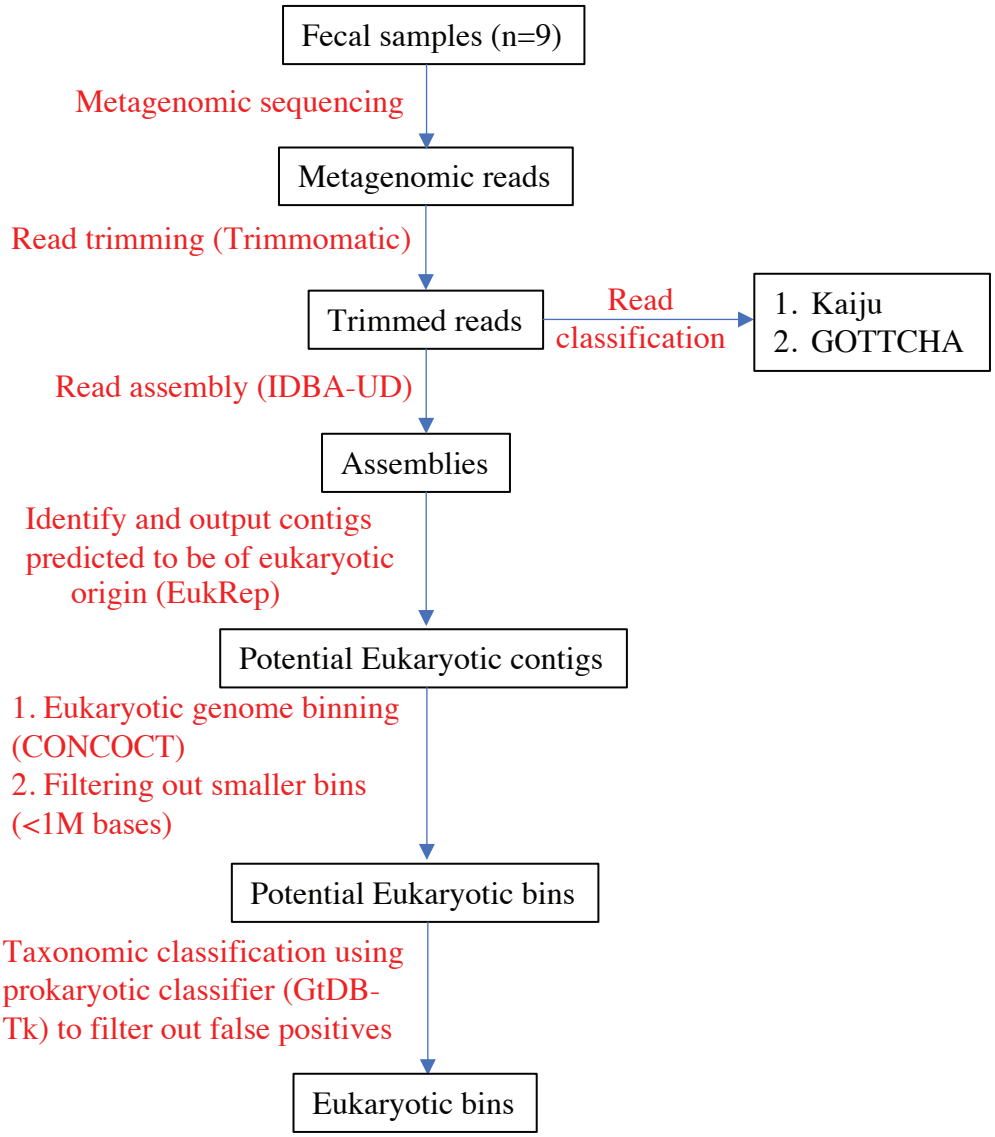
Fecal samples (n=9)
Metagenomic sequencing
Metagenomic reads
Read trimming (Trimmomatic)
Trimmed reads
Read classification
1. Kaiju
2. GOTTCHA
Read assembly (IDBA-UD)
Assemblies
Identify and output contigs predicted to be of eukaryotic origin (EukRep)
Potential Eukaryotic contigs
1. Eukaryotic genome binning (CONCOCT)
2. Filtering out smaller bins (<1M bases)
Potential Eukaryotic bins
Taxonomic classification using prokaryotic classifier (GtDB-Tk) to filter out false positives
Eukaryotic bins

**Supplementary tables.**

**Table S1. Summary of previous high throughput culture-independent studies examining AGF diversity in herbivores.**

**Table S1. Summary of previous high throughput culture-independent studies examining AGF diversity in herbivores.**

| Reference | Location | Sample type | Sequencing Method | Locus | Total number of sequences | Animals studied | | | | | | | |
|---|---|---|---|---|---|---|---|---|---|---|---|---|---|
| | | | | | | Cows (genus Bos) | Horses (including ponies) | Sheep | Goat | Donkey/mule | Deer | Others | Total |
| **Edwards, et al. 2020a** | Europe, Netherlands, Wageningen | Feces | Illumina | ITS1 | ~320K | | | | | 24 | | | 24 |
| **Guo, et al. 2020** | Asia, China, Gansu Province | Rumen | Illumina | ITS1 | ~1.5M | | | 12 | | | | 6 (Yaks) | 18 |
| **Edwards, et al. 2020b** | Europe, Netherlands, Wageningen | Feces | Illumina | ITS1 | NA | | 15 | | | 36 | | 13 (zebra) | 64 |
| **Kittelmann, et al. 2013** | Oceania, New Zealand, Palmerston North, New Zealand, | Rumen | Pyrosequencing | ITS1 | ~72K | 4 | | 5 | | | 2 | | 11 |
| **Kumar, et al. 2015** | North America, United Sattes, PA | Rumen | Pyrosequencing | ITS1 | ~36K | 10 | | | | | | | 10 |
| **Azad, et al. 2020** | North America, Canada, Lethbridge | Rumen | Illumina | ITS1 | ~6.6M | 12 | | | | | | | 12 |
| **Fliegerova, et al. 2021** | South America, Argentina, Mendoza City | Rumen | Illumina, Sanger | ITS2, ITS1 (clones), LSU (one sample, clones) | 413 ITS1 clones, 35 LSU clones, ~534K Illumina | | | | 4 | | | | 4 |
| **Liggenstoffer, et al. 2010** | North America, United States, Oklahoma City | Feces | Pyrosequencing | ITS1 | ~270K | 1 | 3 | 1 | 1 | 2 | 5 | 17 (multiple animals) | 30 |
| **Hanafy, et al. 2020** | North America, United States, Oklahoma and Texas | Feces | SMRT | D1/D2 LSU | ~18K | 2 | 1 | 1 | 1 | | 4 | 12 (multiple animals) | 21 |


**Edwards JE, Schennink A, Burden F, Long S, van Doorn DA et al.** Domesticated equine species and their derived hybrids differ in their fecal microbiota. *Anim Microbiome* 2020a;2:8.
**Guo W, Wang W, Bi S, Long R, Ullah F et al.** Characterization of Anaerobic Rumen Fungal Community Composition in Yak, Tibetan Sheep and Small Tail Han Sheep Grazing on the Qinghai-Tibetan Plateau. *Animals* 2020;10:144.
**Edwards JE, Shetty SA, van den Berg P, Burden F, van Doorn DA et al.** Multi-kingdom characterization of the core equine fecal microbiota based on multiple equine (sub)species. *Anim Microbiome* 2020b;2:6.
**Kittelmann S, Seedorf H, Walters WA, Clemente JC, Knight R et al.** Simultaneous amplicon sequencing to explore co-occurrence patterns of bacterial, archaeal and eukaryotic microorganisms in rumen microbial communities. *PLOS ONE* 2013;8:e47879.
**Kumar S, Indugu N, Vecchiarelli B, Pitta DW**. Associative patterns among anaerobic fungi, methanogenic archaea, and bacterial communities in response to changes in diet and age in the rumen of dairy cows. *Front Microbiol*, 2015;6:781.
**Azad E, Fehr KB, Derakhshani H, Forster R, Acharya S et al.** Interrelationships of fiber-associated anaerobic fungi and bacterial communities in the rumen of bloated cattle grazing alfalfa. *Microorganisms* 2020;8:1543.
**Fliegerova KO, Podmirseg SM, Vinzelj J, Grilli DJ, Kvasnová S et al.** The effect of a high-grain diet on the rumen microbiome of goats with a special focus on anaerobic fungi. *Microorganisms* 2021;9:157.
**Liggenstoffer AS, Youssef NH, Couger MB, Elshahed MS**. Phylogenetic diversity and community structure of anaerobic gut fungi (phylum Neocallimastigomycota) in ruminant and non-ruminant herbivores. *ISME J* 2010;4:1225-1235.
**Hanafy RA, Johnson B, Youssef NH, Elshahed MS**. Assessing anaerobic gut fungal diversity in herbivores using D1/D2 large ribosomal subunit sequencing and multi-year isolation. *Environ Microbiol* 2020;22:3883-3908.

**Table S2 (provided as a separate Excel sheet): Metadata on all 661 datasets examined in this study. Samples are grouped by their gut type, then animal host family, then animal host species. Country of origin (and state within USA), domestication status, and various metadata (including feed type, sex, and age) are also shown. Samples on which additional SMRT sequencing was conducted are highlighted in Red.**

**Table S3 (provided as a separate Excel sheet). AGF genus-level community composition and Good's coverage for the datasets studied. Samples are shown in the same order as in Table S2. Samples on which additional SMRT sequencing was conducted are highlighted in Red.**

**Table S4. Results of Wilcoxon test of significance for the distribution of the percentage of novel genera between different animal species (A), animal families (B), animal gut types (C), domestication status (D), and frequency of study (E).**

Wilcoxon two-sided, adjusted p-value: ns, not significant (p >0.05); *, 0.01 < p < 0.05; **, p < 0.01; ***, p < 0.001; ****, p < 0.0001.

**A**

| Group1 | Group2 | p-value | Sig. level | group1 | group2 | p-value | Sig. level | Group1 | Group2 | p-value | Sig. level |
|---|---|---|---|---|---|---|---|---|---|---|---|
| Alpaca | Horse | 0.023 | * | Capybara | Goat | 0.026 | * | Elephant | Goat | 1.7E-07 | **** |
| | Elephant | 0.046 | * | Chamois | Elephant | 0.038 | * | | Sheep | 7.7E-07 | **** |
| Bison | Elephant | 0.001 | ** | Cattle | Goat | 3.1E-13 | **** | | Yak | 0.003 | ** |
| | Deer | 0.013 | * | | Horse | 8.9E-11 | **** | | Oryx | 0.006 | ** |
| | Goat | 0.014 | * | | Elephant | 1.2E-06 | **** | | Mara | 0.019 | * |
| | Mule | 0.018 | * | | Deer | 3.8E-05 | **** | | Manatee | 0.038 | * |
| | Camel | 0.043 | * | | Sheep | 0.0008 | *** | Elk | Sheep | 0.019 | * |
| Buffalo | Elephant | 1.5E-05 | **** | | Mule | 0.002 | ** | | Goat | 0.024 | * |
| | Horse | 0.0005 | *** | | Mara | 0.015 | * | Giraffe | Sheep | 0.026 | * |
| | Mule | 0.007 | ** | | Donkey | 0.019 | * | | Goat | 0.03 | * |
| | Camel | 0.013 | * | | Elk | 0.019 | * | Goat | Sheep | 8.2E-08 | **** |
| | Donkey | 0.013 | * | | Giraffe | 0.042 | * | | Mule | 0.002 | ** |
| | Elk | 0.026 | * | Deer | Horse | 2.5E-09 | **** | | Mara | 0.016 | * |
| | Mara | 0.026 | * | | Elephant | 1.7E-08 | **** | | Miniature Zebu | 0.018 | * |
| Camel | Deer | 1.2E-05 | **** | | Sheep | 0.0003 | *** | Horse | Sheep | 4.8E-11 | **** |
| | Goat | 0.0001 | *** | | Mule | 0.002 | ** | | Mara | 0.015 | * |
| | Sheep | 0.0001 | *** | | Elk | 0.006 | ** | | Yak | 0.031 | * |
| | Elephant | 0.0006 | *** | | Mara | 0.006 | ** | | Manatee | 0.041 | * |
| | Mule | 0.013 | * | | Miniature Zebu | 0.007 | ** | Mara | Sheep | 0.017 | * |
| | Yak | 0.024 | * | | Giraffe | 0.011 | * | Miniature Zebu | Sheep | 0.015 | * |
| | Cattle | 0.027 | * | | Goat | 0.029 | * | Mule | Sheep | 0.001 | ** |
| | Elk | 0.03 | * | | Donkey | 0.031 | * | | Yak | 0.03 | * |
| | Manatee | 0.03 | * | Donkey | Goat | 0.008 | ** | | | | |
| | Mara | 0.03 | * | | Sheep | 0.024 | * | | | | |

**B**

| Group1 | Group2 | p-value | Sig. level |
|---|---|---|---|
| Bovidae | Equidae | < 2E-16 | **** |
| | Elephantidae | 3.2E-07 | **** |
| | Giraffidae | 0.007 | ** |
| | Cervidae | 0.039 | * |
| Camelidae | Elephantidae | 0.0004 | *** |
| | Cervidae | 0.015 | * |
| | Equidae | 0.018 | * |
| | Giraffidae | 0.026 | * |
| Cervidae | Equidae | 2.1E-08 | **** |
| | Elephantidae | 1.2E-06 | **** |
| | Giraffidae | 0.012 | * |
| Elephantidae | Trichechidae | 0.038 | * |
| Equidae | Trichechidae | 0.042 | * |

**C**

| Group1 | Group2 | p-value | Sig. level |
|---|---|---|---|
| Pseudoruminant | Ruminant | 0.057 | ns |
| | Hindgut | 0.022 | * |
| Ruminant | Hindgut | <2e-16 | **** |

**D**

| Group1 | Group2 | p-value | Sig. level |
|---|---|---|---|
| Domesticated | Non-domesticated | 0.69 | ns |

**E**

| Group1 | Group2 | p-value | Sig. level |
|---|---|---|---|
| Rarely/ never studied | Well studied | 2.30E-10 | **** |

**Table S5. Distribution patterns of novel genera identified in this study*.**

**Table S5. Distribution patterns of novel genera identified in this study.***

| Ubiquity pattern | Relative abundance pattern | Novel genus | No. of samples with abundance | | | | Total number of samples |
|---|---|---|---|---|---|---|---|
| | | | <10% | 10-25% | 25-50% | >50% | |
| **Ubiquitous** (present in >50% of the samples) | **Frequently abundant** (abundance >10% of the community in >5% of the samples they were encountered) | NY44 | 445 | 14 | 3 | 4 | 466 |
| | | NY47 | 351 | 11 | 7 | 3 | 372 |
| | **Rarely abundant** (abundance >10% of the community in < 5% of the samples they were encountered) | NY9 | 484 | 4 | 1 | 0 | 489 |
| | | NY42 | 423 | 5 | 0 | 0 | 428 |
| | | NY1 | 425 | 1 | 0 | 2 | 428 |
| | | NY20 | 357 | 1 | 1 | 1 | 360 |
| | | NY53 | 416 | 1 | 0 | 0 | 417 |
| | | NY15 | 403 | 0 | 1 | 0 | 404 |
| | | NY11 | 399 | 0 | 0 | 1 | 400 |
| | | NY10 | 384 | 1 | 0 | 0 | 385 |
| | | NY17 | 367 | 1 | 0 | 0 | 368 |
| | **Always rare** (abundance < 10% in all of the samples they are encountered) | NY7 | 487 | 0 | 0 | 0 | 487 |
| | | NY8 | 450 | 0 | 0 | 0 | 450 |
| | | NY6 | 440 | 0 | 0 | 0 | 440 |
| | | NY4 | 439 | 0 | 0 | 0 | 439 |
| | | NY19 | 420 | 0 | 0 | 0 | 420 |
| | | NY28 | 397 | 0 | 0 | 0 | 397 |
| | | NY52 | 392 | 0 | 0 | 0 | 392 |
| | | NY21 | 369 | 0 | 0 | 0 | 369 |
| | | NY23 | 367 | 0 | 0 | 0 | 367 |
| | | NY22 | 366 | 0 | 0 | 0 | 366 |
| | | NY55 | 351 | 0 | 0 | 0 | 351 |
| | | NY5 | 346 | 0 | 0 | 0 | 346 |
| | | NY24 | 340 | 0 | 0 | 0 | 340 |
| | | NY2 | 338 | 0 | 0 | 0 | 338 |
| | | NY16 | 333 | 0 | 0 | 0 | 333 |
| | | NY35 | 331 | 0 | 0 | 0 | 331 |
| **Moderately Ubiquitous** (encountered in 10-50% of samples) | **Rarely abundant** (abundance >10% of the community in < 5% of the samples they were encountered) | NY13 | 315 | 1 | 0 | 0 | 316 |
| | **Always rare** (abundance < 10% in all of the samples they are encountered) | NY46 | 325 | 0 | 0 | 0 | 325 |
| | | NY25 | 325 | 0 | 0 | 0 | 325 |
| | | NY50 | 314 | 0 | 0 | 0 | 314 |
| | | NY34 | 301 | 0 | 0 | 0 | 301 |
| | | NY32 | 299 | 0 | 0 | 0 | 299 |
| | | NY54 | 288 | 0 | 0 | 0 | 288 |
| | | NY3 | 272 | 0 | 0 | 0 | 272 |
| | | NY18 | 262 | 0 | 0 | 0 | 262 |
| | | NY26 | 254 | 0 | 0 | 0 | 254 |
| | | NY49 | 226 | 0 | 0 | 0 | 226 |
| | | NY14 | 218 | 0 | 0 | 0 | 218 |
| | | NY48 | 214 | 0 | 0 | 0 | 214 |
| | | NY51 | 200 | 0 | 0 | 0 | 200 |
| | | NY29 | 184 | 0 | 0 | 0 | 184 |
| | | NY33 | 144 | 0 | 0 | 0 | 144 |
| | | NY27 | 144 | 0 | 0 | 0 | 144 |
| | | NY30 | 130 | 0 | 0 | 0 | 130 |
| | | NY37 | 121 | 0 | 0 | 0 | 121 |
| | | NY12 | 104 | 0 | 0 | 0 | 104 |
| **Not ubiquitous** (present in <10% of the samples) | **Always rare** (abundance < 10% in all of the samples they are encountered) | NY40 | 56 | 0 | 0 | 0 | 56 |
| | | NY45 | 46 | 0 | 0 | 0 | 46 |
| | | NY31 | 39 | 0 | 0 | 0 | 39 |
| | | NY39 | 26 | 0 | 0 | 0 | 26 |
| | | NY41 | 14 | 0 | 0 | 0 | 14 |
| | | NY38 | 9 | 0 | 0 | 0 | 9 |
| | | NY56 | 7 | 0 | 0 | 0 | 7 |
| | | NY43 | 5 | 0 | 0 | 0 | 5 |
| | | NY36 | 3 | 0 | 0 | 0 | 3 |

*Genera were first classified as ubiquitous, moderately ubiquitous, and not ubiquitous. Within these classifications, genera percentage abundance in their respective samples was used to further classify them into frequently abundant, rarely abundant, or always rare. Two novel genera were ubiquitous and frequently abundant, NY47 and NY44, and were both present in high abundance in goats, with occasional high abundance of NY47 in sheep, and occasional high abundance of NY44 in alpaca. Nine genera were ubiquitous but rarely abundant, including NY1, which constituted the absolute majority of the community in the two mara samples, the genera NY15, and NY20 that accounted for 41.8%, and 98.7%, respectively in two rhinoceros' samples, and NY11 that accounted for 60% of the community in one chamois sample. Sixteen novel genera were ubiquitous but always rare. One genus, NY13, was moderately ubiquitous but rarely abundant, where it constituted 11.7% of the community in a single cow sample but made up a minor fraction of the community in all other samples where it was identified (n=315). Nineteen of the 56 novel genera were moderately ubiquitous but always rare, while 8 genera were not ubiquitous and always rare.

**Table S6. PacBio-generated sequences belonging to 49 of the 56 novel genera generated in this study, their novel genus affiliation, and their corresponding GenBank accession number.**

**Table S6. PacBio-generated sequences belonging to 49 of the 56 novel genera identified in this study, their novel genus affiliation, and the corresponding GenBank accession number.**

| Sequence name | Novel genus Affiliation | GenBank accession number |
|---|---|---|
| NY01_m54363_210702_230832/43254648/ccs | NY01 | OP253744 |
| NY01_m54363_210715_173500/14287146/ccs | NY01 | OP253711 |
| NY01_m54363_210715_173500/27394924/ccs | NY01 | OP253712 |
| NY01_m54363_210715_173500/38535703/ccs | NY01 | OP253713 |
| NY01_m54363_210715_173500/54460758/ccs | NY01 | OP253714 |
| NY02_m54363_210702_230832/15664056/ccs | NY02 | OP253743 |
| NY02_m54363_210702_230832/53543131/ccs | NY02 | OP253745 |
| NY02_m54363_210715_173500/24117532/ccs | NY02 | OP253803 |
| NY02_m54363_210715_173500/24838808/ccs | NY02 | OP253804 |
| NY02_m54363_210715_173500/50725528/ccs | NY02 | OP253805 |
| NY03_m54363_210702_230832/10092648/ccs | NY03 | OP253846 |
| NY03_m54363_210702_230832/48234667/ccs | NY03 | OP253850 |
| NY03_m54363_210702_230832/60490277/ccs | NY03 | OP253847 |
| NY03_m54363_210715_173500/24379683/ccs | NY03 | OP253848 |
| NY03_m54363_210715_173500/24969633/ccs | NY03 | OP253849 |
| NY03_m54363_210715_173500/26476964/ccs | NY03 | OP253746 |
| NY03_m54363_210715_173500/66060421/ccs | NY03 | OP253851 |
| NY04_m54363_210702_230832/17236627/ccs | NY04 | OP253863 |
| NY04_m54363_210702_230832/18416025/ccs | NY04 | OP253864 |
| NY04_m54363_210702_230832/71893603/ccs | NY04 | OP253865 |
| NY04_m54363_210715_173500/25428967/ccs | NY04 | OP253747 |
| NY05_m54363_210702_230832/31588788/ccs | NY05 | OP253911 |
| NY05_m54363_210702_230832/40763577/ccs | NY05 | OP253912 |
| NY05_m54363_210702_230832/70189921/ccs | NY05 | OP253913 |
| NY05_m54363_210702_230832/74908399/ccs | NY05 | OP253748 |
| NY05_m54363_210715_173500/43451173/ccs | NY05 | OP253914 |
| NY06_m54363_210702_230832/26018351/ccs | NY06 | OP253749 |
| NY06_m54363_210702_230832/63504478/ccs | NY06 | OP253928 |
| NY06_m54363_210715_173500/18546851/ccs | NY06 | OP253929 |
| NY06_m54363_210715_173500/44958340/ccs | NY06 | OP253930 |
| NY06_m54363_210715_173500/9569081/ccs | NY06 | OP253750 |
| NY07_m54363_210702_230832/29360628/ccs | NY07 | OP253931 |
| NY07_m54363_210715_173500/19464266/ccs | NY07 | OP253751 |
| NY07_m54363_210715_173500/21496290/ccs | NY07 | OP253932 |
| NY07_m54363_210715_173500/28312294/ccs | NY07 | OP253933 |
| NY07_m54363_210715_173500/66126471/ccs | NY07 | OP253934 |
| NY08_m54363_210702_230832/50659587/ccs | NY08 | OP253935 |
| NY08_m54363_210702_230832/62456101/ccs | NY08 | OP253752 |
| NY08_m54363_210715_173500/28377300/ccs | NY08 | OP253937 |
| NY08_m54363_210715_173500/34406930/ccs | NY08 | OP253938 |
| NY08_m54363_210715_173500/50922425/ccs | NY08 | OP253939 |
| NY08_m54363_210715_173500/61408089/ccs | NY08 | OP253936 |
| NY09_m54363_210702_230832/19661621/ccs | NY09 | OP253952 |
| NY09_m54363_210702_230832/27132876/ccs | NY09 | OP253953 |
| NY09_m54363_210702_230832/4390984/ccs | NY09 | OP253944 |
| NY09_m54363_210702_230832/55247133/ccs | NY09 | OP253945 |
| NY09_m54363_210702_230832/56099373/ccs | NY09 | OP253940 |
| NY09_m54363_210715_173500/21234182/ccs | NY09 | OP253753 |

| | | |
|---|---|---|
| NY09_m54363_210715_173500/23331195/ccs | NY09 | OP253946 |
| NY09_m54363_210715_173500/31261493/ccs | NY09 | OP253948 |
| NY09_m54363_210715_173500/39256976/ccs | NY09 | OP253949 |
| NY09_m54363_210715_173500/44040288/ccs | NY09 | OP253754 |
| NY09_m54363_210715_173500/44368621/ccs | NY09 | OP253947 |
| NY09_m54363_210715_173500/44434278/ccs | NY09 | OP253954 |
| NY09_m54363_210715_173500/44630853/ccs | NY09 | OP253755 |
| NY09_m54363_210715_173500/44827596/ccs | NY09 | OP253941 |
| NY09_m54363_210715_173500/47055612/ccs | NY09 | OP253942 |
| NY09_m54363_210715_173500/50660050/ccs | NY09 | OP253756 |
| NY09_m54363_210715_173500/54919854/ccs | NY09 | OP253955 |
| NY09_m54363_210715_173500/55247788/ccs | NY09 | OP253943 |
| NY09_m54363_210715_173500/70713887/ccs | NY09 | OP253950 |
| NY09_m54363_210715_173500/7930439/ccs | NY09 | OP253951 |
| NY10_m54363_210702_230832/19530507/ccs | NY10 | OP253715 |
| NY10_m54363_210702_230832/25887602/ccs | NY10 | OP253719 |
| NY10_m54363_210702_230832/57016793/ccs | NY10 | OP253716 |
| NY10_m54363_210715_173500/23397130/ccs | NY10 | OP253720 |
| NY10_m54363_210715_173500/34537950/ccs | NY10 | OP253717 |
| NY10_m54363_210715_173500/68616855/ccs | NY10 | OP253718 |
| NY10_m54363_210715_173500/73532069/ccs | NY10 | OP253757 |
| NY11_m54363_210702_230832/48366062/ccs | NY11 | OP253758 |
| NY11_m54363_210715_173500/25559925/ccs | NY11 | OP253721 |
| NY11_m54363_210715_173500/30999471/ccs | NY11 | OP253722 |
| NY11_m54363_210715_173500/35848503/ccs | NY11 | OP253723 |
| NY11_m54363_210715_173500/54198980/ccs | NY11 | OP253724 |
| NY12_m54363_210702_230832/33293210/ccs | NY12 | OP253725 |
| NY12_m54363_210702_230832/61603955/ccs | NY12 | OP253759 |
| NY12_m54363_210702_230832/67764685/ccs | NY12 | OP253726 |
| NY12_m54363_210715_173500/15270300/ccs | NY12 | OP253727 |
| NY12_m54363_210715_173500/58328007/ccs | NY12 | OP253728 |
| NY13_m54363_210702_230832/18154450/ccs | NY13 | OP253760 |
| NY13_m54363_210702_230832/20709469/ccs | NY13 | OP253729 |
| NY13_m54363_210702_230832/47186009/ccs | NY13 | OP253730 |
| NY14_m54363_210715_173500/53412712/ccs | NY14 | OP253761 |
| NY14_m54363_210715_173500/63046527/ccs | NY14 | OP253731 |
| NY14_m54363_210715_173500/63701493/ccs | NY14 | OP253732 |
| NY15_m54363_210702_230832/48431561/ccs | NY15 | OP253733 |
| NY15_m54363_210715_173500/12190260/ccs | NY15 | OP253734 |
| NY15_m54363_210715_173500/35193328/ccs | NY15 | OP253762 |
| NY16_m54363_210702_230832/16450074/ccs | NY16 | OP253735 |
| NY16_m54363_210715_173500/24379841/ccs | NY16 | OP253763 |
| NY16_m54363_210715_173500/44696278/ccs | NY16 | OP253736 |
| NY16_m54363_210715_173500/9240892/ccs | NY16 | OP253737 |
| NY17_m54363_210702_230832/13435704/ccs | NY17 | OP253764 |
| NY17_m54363_210715_173500/17170706/ccs | NY17 | OP253738 |
| NY17_m54363_210715_173500/6488806/ccs | NY17 | OP253739 |
| NY17_m54363_210715_173500/66585386/ccs | NY17 | OP253740 |
| NY18_m54363_210702_230832/53805634/ccs | NY18 | OP253741 |
| NY18_m54363_210715_173500/56623301/ccs | NY18 | OP253765 |
| NY19_m54363_210702_230832/71893205/ccs | NY19 | OP253742 |

| | | |
|---|---|---|
| NY19_m54363_210715_173500/59900679/ccs | NY19 | OP253766 |
| NY20_m54363_210702_230832/44695989/ccs | NY20 | OP253806 |
| NY20_m54363_210702_230832/72483236/ccs | NY20 | OP253767 |
| NY20_m54363_210715_173500/70583178/ccs | NY20 | OP253807 |
| NY21_m54363_210702_230832/15073783/ccs | NY21 | OP253808 |
| NY21_m54363_210702_230832/69993298/ccs | NY21 | OP253768 |
| NY21_m54363_210715_173500/50331792/ccs | NY21 | OP253809 |
| NY21_m54363_210715_173500/6619609/ccs | NY21 | OP253810 |
| NY22_m54363_210702_230832/18088952/ccs | NY22 | OP253769 |
| NY22_m54363_210715_173500/19726933/ccs | NY22 | OP253811 |
| NY22_m54363_210715_173500/31261216/ccs | NY22 | OP253812 |
| NY22_m54363_210715_173500/65339627/ccs | NY22 | OP253813 |
| NY22_m54363_210715_173500/67633344/ccs | NY22 | OP253814 |
| NY23_m54363_210702_230832/9699688/ccs | NY23 | OP253815 |
| NY23_m54363_210715_173500/12714678/ccs | NY23 | OP253816 |
| NY23_m54363_210715_173500/22348539/ccs | NY23 | OP253817 |
| NY23_m54363_210715_173500/35455201/ccs | NY23 | OP253818 |
| NY23_m54363_210715_173500/48431264/ccs | NY23 | OP253770 |
| NY24_m54363_210702_230832/65143010/ccs | NY24 | OP253819 |
| NY24_m54363_210702_230832/72352197/ccs | NY24 | OP253820 |
| NY24_m54363_210715_173500/21430925/ccs | NY24 | OP253821 |
| NY24_m54363_210715_173500/45941343/ccs | NY24 | OP253771 |
| NY25_m54363_210702_230832/17040235/ccs | NY25 | OP253772 |
| NY25_m54363_210702_230832/20906881/ccs | NY25 | OP253825 |
| NY25_m54363_210702_230832/41550390/ccs | NY25 | OP253773 |
| NY25_m54363_210702_230832/55116789/ccs | NY25 | OP253822 |
| NY25_m54363_210715_173500/22741554/ccs | NY25 | OP253826 |
| NY25_m54363_210715_173500/53215543/ccs | NY25 | OP253823 |
| NY25_m54363_210715_173500/58655172/ccs | NY25 | OP253827 |
| NY25_m54363_210715_173500/60293669/ccs | NY25 | OP253828 |
| NY25_m54363_210715_173500/60948660/ccs | NY25 | OP253824 |
| NY26_m54363_210702_230832/16973917/ccs | NY26 | OP253774 |
| NY26_m54363_210702_230832/45482088/ccs | NY26 | OP253829 |
| NY26_m54363_210715_173500/50201294/ccs | NY26 | OP253830 |
| NY26_m54363_210715_173500/53543814/ccs | NY26 | OP253831 |
| NY26_m54363_210715_173500/64225806/ccs | NY26 | OP253832 |
| NY27_m54363_210702_230832/18875316/ccs | NY27 | OP253833 |
| NY27_m54363_210702_230832/55050585/ccs | NY27 | OP253834 |
| NY27_m54363_210715_173500/24838516/ccs | NY27 | OP253835 |
| NY27_m54363_210715_173500/28443603/ccs | NY27 | OP253775 |
| NY27_m54363_210715_173500/57934202/ccs | NY27 | OP253836 |
| NY28_m54363_210702_230832/44827451/ccs | NY28 | OP253837 |
| NY28_m54363_210715_173500/13435796/ccs | NY28 | OP253838 |
| NY28_m54363_210715_173500/49808149/ccs | NY28 | OP253839 |
| NY28_m54363_210715_173500/67829881/ccs | NY28 | OP253776 |
| NY28_m54363_210715_173500/72810716/ccs | NY28 | OP253840 |
| NY29_m54363_210702_230832/73531944/ccs | NY29 | OP253844 |
| NY29_m54363_210715_173500/29557232/ccs | NY29 | OP253777 |
| NY29_m54363_210715_173500/4849974/ccs | NY29 | OP253841 |
| NY29_m54363_210715_173500/50659812/ccs | NY29 | OP253842 |
| NY29_m54363_210715_173500/5898937/ccs | NY29 | OP253778 |

| | | |
|---|---|---|
| NY29_m54363_210715_173500/68420521/ccs | NY29 | OP253845 |
| NY29_m54363_210715_173500/9831322/ccs | NY29 | OP253843 |
| NY30_m54363_210715_173500/61342497/ccs | NY30 | OP253779 |
| NY33_m54363_210702_230832/37094118/ccs | NY33 | OP253852 |
| NY33_m54363_210702_230832/39321839/ccs | NY33 | OP253780 |
| NY33_m54363_210702_230832/40371130/ccs | NY33 | OP253853 |
| NY33_m54363_210702_230832/46006950/ccs | NY33 | OP253854 |
| NY33_m54363_210715_173500/18350935/ccs | NY33 | OP253855 |
| NY34_m54363_210702_230832/10224104/ccs | NY34 | OP253856 |
| NY34_m54363_210715_173500/46990047/ccs | NY34 | OP253857 |
| NY34_m54363_210715_173500/66781632/ccs | NY34 | OP253781 |
| NY34_m54363_210715_173500/72679691/ccs | NY34 | OP253858 |
| NY35_m54363_210702_230832/30016443/ccs | NY35 | OP253859 |
| NY35_m54363_210702_230832/66650513/ccs | NY35 | OP253860 |
| NY35_m54363_210715_173500/57213867/ccs | NY35 | OP253861 |
| NY35_m54363_210715_173500/66977901/ccs | NY35 | OP253782 |
| NY35_m54363_210715_173500/70189294/ccs | NY35 | OP253862 |
| NY36_m54363_210702_230832/19792477/ccs | NY36 | OP253956 |
| NY42_m54363_210702_230832/16450240/ccs | NY42 | OP253866 |
| NY42_m54363_210702_230832/20185441/ccs | NY42 | OP253783 |
| NY42_m54363_210702_230832/27394288/ccs | NY42 | OP253873 |
| NY42_m54363_210702_230832/33293249/ccs | NY42 | OP253870 |
| NY42_m54363_210702_230832/45809815/ccs | NY42 | OP253784 |
| NY42_m54363_210702_230832/48496900/ccs | NY42 | OP253874 |
| NY42_m54363_210702_230832/52101855/ccs | NY42 | OP253867 |
| NY42_m54363_210702_230832/69010180/ccs | NY42 | OP253875 |
| NY42_m54363_210715_173500/11011062/ccs | NY42 | OP253871 |
| NY42_m54363_210715_173500/16974331/ccs | NY42 | OP253868 |
| NY42_m54363_210715_173500/43516478/ccs | NY42 | OP253876 |
| NY42_m54363_210715_173500/43712632/ccs | NY42 | OP253869 |
| NY42_m54363_210715_173500/50135339/ccs | NY42 | OP253872 |
| NY42_m54363_210715_173500/6619941/ccs | NY42 | OP253785 |
| NY43_m54363_210702_230832/39911764/ccs | NY43 | OP253877 |
| NY43_m54363_210702_230832/53281643/ccs | NY43 | OP253878 |
| NY43_m54363_210715_173500/51184427/ccs | NY43 | OP253786 |
| NY43_m54363_210715_173500/57147735/ccs | NY43 | OP253879 |
| NY43_m54363_210715_173500/73990289/ccs | NY43 | OP253880 |
| NY44_m54363_210702_230832/10748553/ccs | NY44 | OP253887 |
| NY44_m54363_210702_230832/13828712/ccs | NY44 | OP253888 |
| NY44_m54363_210702_230832/17891559/ccs | NY44 | OP253889 |
| NY44_m54363_210702_230832/49808338/ccs | NY44 | OP253886 |
| NY44_m54363_210702_230832/60883409/ccs | NY44 | OP253787 |
| NY44_m54363_210702_230832/66257220/ccs | NY44 | OP253891 |
| NY44_m54363_210702_230832/73072783/ccs | NY44 | OP253885 |
| NY44_m54363_210715_173500/11534972/ccs | NY44 | OP253892 |
| NY44_m54363_210715_173500/14877433/ccs | NY44 | OP253788 |
| NY44_m54363_210715_173500/44565298/ccs | NY44 | OP253881 |
| NY44_m54363_210715_173500/51445867/ccs | NY44 | OP253893 |
| NY44_m54363_210715_173500/54526651/ccs | NY44 | OP253789 |
| NY44_m54363_210715_173500/54526828/ccs | NY44 | OP253882 |
| NY44_m54363_210715_173500/55772139/ccs | NY44 | OP253890 |

| | | |
|---|---|---|
| NY44_m54363_210715_173500/56427083/ccs | NY44 | OP253790 |
| NY44_m54363_210715_173500/64684567/ccs | NY44 | OP253883 |
| NY44_m54363_210715_173500/66716539/ccs | NY44 | OP253894 |
| NY44_m54363_210715_173500/67371233/ccs | NY44 | OP253791 |
| NY44_m54363_210715_173500/69010279/ccs | NY44 | OP253884 |
| NY45_m54363_210702_230832/40436554/ccs | NY45 | OP253895 |
| NY45_m54363_210702_230832/70386240/ccs | NY45 | OP253896 |
| NY45_m54363_210702_230832/73269706/ccs | NY45 | OP253897 |
| NY45_m54363_210715_173500/17891797/ccs | NY45 | OP253792 |
| NY46_m54363_210702_230832/57279149/ccs | NY46 | OP253898 |
| NY46_m54363_210702_230832/59506918/ccs | NY46 | OP253793 |
| NY46_m54363_210702_230832/68223892/ccs | NY46 | OP253899 |
| NY46_m54363_210715_173500/17236524/ccs | NY46 | OP253900 |
| NY47_m54363_210702_230832/12583354/ccs | NY47 | OP253902 |
| NY47_m54363_210702_230832/33096050/ccs | NY47 | OP253903 |
| NY47_m54363_210702_230832/4588143/ccs | NY47 | OP253901 |
| NY47_m54363_210702_230832/63177338/ccs | NY47 | OP253794 |
| NY47_m54363_210715_173500/64815726/ccs | NY47 | OP253904 |
| NY47_m54363_210715_173500/6685291/ccs | NY47 | OP253795 |
| NY47_m54363_210715_173500/67568477/ccs | NY47 | OP253905 |
| NY48_m54363_210702_230832/66322747/ccs | NY48 | OP253906 |
| NY48_m54363_210702_230832/68288683/ccs | NY48 | OP253907 |
| NY48_m54363_210715_173500/21037281/ccs | NY48 | OP253908 |
| NY48_m54363_210715_173500/39191176/ccs | NY48 | OP253909 |
| NY48_m54363_210715_173500/56950989/ccs | NY48 | OP253796 |
| NY49_m54363_210702_230832/63767382/ccs | NY49 | OP253797 |
| NY49_m54363_210715_173500/72548810/ccs | NY49 | OP253910 |
| NY50_m54363_210702_230832/59114097/ccs | NY50 | OP253915 |
| NY50_m54363_210715_173500/18612605/ccs | NY50 | OP253916 |
| NY50_m54363_210715_173500/48234766/ccs | NY50 | OP253798 |
| NY51_m54363_210715_173500/51052739/ccs | NY51 | OP253799 |
| NY52_m54363_210702_230832/56361315/ccs | NY52 | OP253917 |
| NY52_m54363_210702_230832/65143181/ccs | NY52 | OP253918 |
| NY52_m54363_210715_173500/48104031/ccs | NY52 | OP253800 |
| NY52_m54363_210715_173500/67371722/ccs | NY52 | OP253919 |
| NY53_m54363_210702_230832/22282617/ccs | NY53 | OP253920 |
| NY53_m54363_210702_230832/66388768/ccs | NY53 | OP253801 |
| NY53_m54363_210715_173500/26149186/ccs | NY53 | OP253921 |
| NY53_m54363_210715_173500/47645621/ccs | NY53 | OP253922 |
| NY53_m54363_210715_173500/52560584/ccs | NY53 | OP253923 |
| NY54_m54363_210702_230832/42927017/ccs | NY54 | OP253960 |
| NY54_m54363_210702_230832/14942767/ccs | NY54 | OP253963 |
| NY54_m54363_210702_230832/67961557/ccs | NY54 | OP253961 |
| NY54_m54363_210715_173500/38470488/ccs | NY54 | OP253962 |
| NY55_m54363_210702_230832/13107420/ccs | NY55 | OP253924 |
| NY55_m54363_210702_230832/29688374/ccs | NY55 | OP253925 |
| NY55_m54363_210702_230832/54132989/ccs | NY55 | OP253926 |
| NY55_m54363_210715_173500/40370257/ccs | NY55 | OP253927 |
| NY55_m54363_210715_173500/68027297/ccs | NY55 | OP253802 |
| NY56_m54363_210715_173500/32243954/ccs | NY56 | OP253959 |

**Table S7. Topology comparison between trees constructed using Illumina-generated sequences affiliated with novel genera versus SMRT-generated sequences affiliated with novel genera.** The novel genera are color coded to reflect congruency between the two trees (yellow, positions congruent; green, positions non-congruent). Blue highlights the 7 novel genera that were missing from the PacBio dataset. These genera exhibited an extremely rare occurrence in the corresponding Illumina-sequenced samples (never exceeding 0.1% in any of the 61 samples) as well as the total dataset (abundances ranging between 0.0004-0.07% in the total Illumina dataset).

**Table S7. Topology comparison between trees constructed using Illumina-generated sequences affiliated with novel genera versus SMRT-generated sequences affiliated with novel genera.**

| Genus | Affiliation/Phylogenetic placement (Illumina tree, Fig 2a) | Affiliation/Phylogenetic placement (SMRT tree, Fig S5) |
|---|---|---|
| NY1 | Family *Caecomycetaceae* | Basal position |
| NY2 | Family *Piromycetaceae* | Family *Piromycetaceae* |
| NY3 | Basal to the families *Caecomycetaceae* and *Piromycetaceae* | Family *Caecomycetaceae* |
| NY4 | Basal to the families *Caecomycetaceae* and *Piromycetaceae* | Family *Caecomycetaceae* |
| NY5 | Family *Piromycetaceae* | Family *Piromycetaceae* |
| NY6 | Family *Neocallimastigaceae* | Family *Caecomycetaceae* |
| NY7 | Family *Neocallimastigaceae* | Family *Neocallimastigaceae* |
| NY8 | Family *Piromycetaceae* | Family *Piromycetaceae* |
| NY9 | Basal to the families *Caecomycetaceae* and *Piromycetaceae* | Basal to the family *Caecomycetaceae* |
| NY10 | Novel family affiliated with *Buwchfawromyces* and *Tahromyces* | Novel family affiliated with *Buwchfawromyces* and *Tahromyces* |
| NY11 | Novel family affiliated with *Buwchfawromyces* and *Tahromyces* | Novel family affiliated with *Buwchfawromyces* and *Tahromyces* |
| NY12 | Family *Anaeromycetaceae* | Family *Anaeromycetaceae* |
| NY13 | Novel family affiliated with *Joblinomyces* | Novel family affiliated with *Joblinomyces* |
| NY14 | Family *Neocallimastigaceae* | Family *Caecomycetaceae* |
| NY15 | Family *Anaeromycetaceae* | Family *Anaeromycetaceae* |
| NY16 | Family *Anaeromycetaceae* | Family *Anaeromycetaceae* |
| NY17 | Family *Anaeromycetaceae* | Family *Anaeromycetaceae* |
| NY18 | Family *Anaeromycetaceae* | Family *Anaeromycetaceae* |
| NY19 | Family *Anaeromycetaceae* | Family *Anaeromycetaceae* |
| NY20 | Family *Anaeromycetaceae* | Family *Anaeromycetaceae* |
| NY21 | Family *Neocallimastigaceae* | Family *Neocallimastigaceae* |
| NY22 | Family *Neocallimastigaceae* | Family *Neocallimastigaceae* |
| NY23 | Family *Neocallimastigaceae* | Family *Neocallimastigaceae* |
| NY24 | Family *Neocallimastigaceae* | Family *Neocallimastigaceae* |
| NY25 | Family *Caecomycetaceae* | Family *Caecomycetaceae* |
| NY26 | Basal to the families *Caecomycetaceae* and *Piromycetaceae* | Family *Caecomycetaceae* |
| NY27 | Family *Caecomycetaceae* | Family *Caecomycetaceae* |
| NY28 | Family *Neocallimastigaceae* | Family *Neocallimastigaceae* |
| NY29 | Family *Neocallimastigaceae* | Family *Neocallimastigaceae* |
| NY30 | Family *Caecomycetaceae* | Family *Caecomycetaceae* |
| NY31 | Basal to the families *Caecomycetaceae* and *Piromycetaceae* | Missing |
| NY32 | Basal to the families *Caecomycetaceae* and *Piromycetaceae* | Missing |
| NY33 | Family *Caecomycetaceae* | Family *Caecomycetaceae* |
| NY34 | Family *Caecomycetaceae* | Family *Caecomycetaceae* |
| NY35 | Family *Caecomycetaceae* | Family *Caecomycetaceae* |
| NY36 | Novel family affiliated with *Khoyollomyces* | Novel family affiliated with *Khoyollomyces* |
| NY37 | Novel family affiliated with *Aklioshbomyces* | Missing |
| NY38 | Novel family affiliated with *Aklioshbomyces* | Missing |
| NY39 | Novel family affiliated with *Aklioshbomyces* | Missing |
| NY40 | Novel family affiliated with *Aklioshbomyces* | Missing |
| NY41 | Novel family affiliated with *Aklioshbomyces* | Missing |
| NY42 | Novel family affiliated with *Buwchfawromyces* and *Tahromyces* | Novel family affiliated with *Buwchfawromyces* and *Tahromyces* |
| NY43 | Novel family affiliated with *Buwchfawromyces* and *Tahromyces* | Novel family affiliated with *Buwchfawromyces* and *Tahromyces* |
| NY44 | Novel family affiliated with *Joblinomyces* | Novel family affiliated with *Joblinomyces* |
| NY45 | Family *Neocallimastigaceae* | Family *Neocallimastigaceae* |
| NY46 | Novel family affiliated with *Joblinomyces* | Novel family affiliated with *Joblinomyces* |
| NY47 | Novel family affiliated with *Joblinomyces* | Novel family affiliated with *Joblinomyces* |
| NY48 | Family *Neocallimastigaceae* | Novel family affiliated with *Joblinomyces* |
| NY49 | Novel family affiliated with *Joblinomyces* | Novel family affiliated with *Joblinomyces* |
| NY50 | Basal to the families *Caecomycetaceae* and *Piromycetaceae* | Family *Anaeromycetaceae* |
| NY51 | Family *Anaeromycetaceae* | Family *Anaeromycetaceae* |
| NY52 | Family *Neocallimastigaceae* | Family *Neocallimastigaceae* |
| NY53 | Family *Neocallimastigaceae* | Family *Neocallimastigaceae* |
| NY54 | Novel family affiliated with *Khoyollomyces* | Novel family affiliated with *Khoyollomyces* |
| NY55 | Family *Anaeromycetaceae* | Family *Anaeromycetaceae* |
| NY56 | Novel family affiliated with *Khoyollomyces* | Novel family affiliated with *Khoyollomyces* |

| Color key |
|---|
| Positions matching in both trees |
| Positions variable |
| Missing from the SMRT tree |

**Table S8.** Values of normalized stochasticity ratios (NST) calculated using the two indices Bray-Curtis and Jaccard.

**Table S8. Values of normalized stochasticity ratios(NST) calculated using two indices.**

| Factor | | Group | $NST_{Bray-Curtis}$ | $NST_{Jaccard}$ |
|---|---|---|---|---|
| Host-associated factors | Gut type | Hindgut | 0.56 | 0.64 |
| | | Foregut Pseudoruminant | 0.77 | 0.58 |
| | | Foregut ruminant | 0.87 | 0.79 |
| | | | | |
| | Animal family | Elephantidae | 0.41 | 0.35 |
| | | Equidae | 0.54 | 0.64 |
| | | Camelidae | 0.78 | 0.58 |
| | | Bovidae | 0.87 | 0.77 |
| | | Cervidae | 0.90 | 0.86 |
| | | | | |
| | Animal species | Horse | 0.52 | 0.65 |
| | | Goat | 0.79 | 0.70 |
| | | Cow | 0.81 | 0.79 |
| | | Sheep | 0.84 | 0.66 |
| | | Deer | 0.95 | 0.83 |
| | | | | |
| Non host-associated factors | Domestication status | Domesticated | 0.79 | 0.77 |
| | | Non-domesticated | 0.76 | 0.75 |

**Table S9. Results of Wilcoxon test of significance for the distribution of PACo residuals between different animal species (A), animal families (B), and animal gut types (C).**

**A**

| Group1 | Group2 | p.adj | p.signif |
|---|---|---|---|
| Alpaca | Bison | 0.011 | ** |
| | Buffalo | 0.0028 | *** |
| | Cattle | 0.0011 | **** |
| | Deer | 8.40E-05 | **** |
| | Donkey | 0.031 | ** |
| | Elephant | 0.0016 | **** |
| | Goat | 0.0014 | **** |
| | Horse | 0.043 | ** |
| | Mule | 0.055 | ** |
| | Oryx | 0.055 | ** |
| | Rhinoceros | 0.09 | * |
| | Sheep | 0.0014 | **** |
| | Yak | 0.055 | ** |
| | Zebra | 0.055 | ** |
| Bison | Camel | 0.0019 | *** |
| | Deer | 0.14 | * |
| | Donkey | 0.021 | ** |
| | Elephant | 0.00065 | **** |
| | Horse | 4.00E-04 | **** |
| | Mule | 0.039 | ** |
| | Rhinoceros | 0.039 | ** |
| | Zebra | 0.039 | ** |
| Buffalo | Camel | 0.00017 | **** |
| | Donkey | 0.0067 | *** |
| | Elephant | 2.80E-05 | **** |
| | Horse | 5.90E-06 | **** |
| | Mule | 0.013 | ** |
| | Rhinoceros | 0.013 | ** |
| | Zebra | 0.013 | ** |
| Camel | Cattle | 1.10E-05 | **** |
| | Deer | 8.20E-07 | **** |
| | Donkey | 0.033 | ** |
| | Goat | 1.80E-05 | **** |
| | Horse | 0.012 | ** |
| | Mule | 0.016 | ** |
| | Oryx | 0.016 | ** |
| | Rhinoceros | 0.049 | ** |
| | Sheep | 2.10E-05 | **** |
| | Yak | 0.016 | ** |
| | Zebra | 0.03 | ** |

| Group1 | Group2 | p.adj | p.signif |
|---|---|---|---|
| Cattle | Deer | 0.013 | ** |
| | Donkey | 0.0032 | *** |
| | Elephant | 6.30E-07 | **** |
| | Horse | 1.10E-23 | **** |
| | Mule | 0.0091 | *** |
| | Rhinoceros | 0.0091 | *** |
| | Zebra | 0.0091 | *** |
| White-tail deer | Donkey | 0.00039 | **** |
| | Elephant | 3.90E-08 | **** |
| | Goat | 0.0082 | *** |
| | Horse | 2.40E-11 | **** |
| | Mule | 0.0016 | **** |
| | Rhinoceros | 0.0016 | **** |
| | Sheep | 0.0039 | *** |
| | Yak | 0.049 | ** |
| | Zebra | 0.0016 | **** |
| Donkey | Elephant | 0.0037 | *** |
| | Goat | 0.0037 | *** |
| | Oryx | 0.089 | * |
| | Sheep | 0.0038 | *** |
| | Yak | 0.089 | * |
| Elephant | Mule | 0.0091 | *** |
| | Oryx | 0.0091 | *** |
| | Rhinoceros | 0.0091 | *** |
| | Yak | 0.0091 | *** |
| | Zebra | 0.0091 | *** |
| Goat | Elephant | 9.90E-07 | **** |
| | Mule | 0.0091 | *** |
| | Rhinoceros | 0.0091 | *** |
| | Zebra | 0.0091 | *** |
| Horse | Elephant | 9.90E-07 | **** |
| | Goat | 1.60E-20 | **** |
| | Oryx | 0.0091 | *** |
| | Yak | 0.0091 | *** |

**B**

| Group1 | Group2 | p.adj | p.signif |
|---|---|---|---|
| Camelidae | Bovidae | 5.10E-11 | **** |
| | Caviidae | 0.00021 | **** |
| | Cervidae | 2.20E-11 | **** |
| | Equidae | 2.30E-05 | **** |
| | Elephantidae | 7.50E-08 | **** |
| | Giraffidae | 0.0033 | ** |
| | Trichechidae | 0.017 | * |
| | Rhinocerotidae | 0.0042 | ** |
| Bovidae | Caviidae | 0.00034 | *** |
| | Cervidae | 0.00011 | **** |
| | Equidae | 3.20E-40 | **** |
| | Elephantidae | 7.60E-09 | **** |
| | Giraffidae | 0.0051 | ** |
| | Trichechidae | 0.021 | * |
| | Rhinocerotidae | 0.0013 | *** |

| Group1 | Group2 | p.adj | p.signif |
|---|---|---|---|
| Cervidae | Equidae | 6.20E-14 | **** |
| | Elephantidae | 8.20E-10 | **** |
| | Giraffidae | 0.001 | *** |
| | Trichechidae | 0.0069 | ** |
| | Rhinocerotidae | 0.00017 | **** |
| Equidae | Elephantidae | 4.70E-08 | **** |
| | Giraffidae | 0.0056 | ** |
| | Trichechidae | 0.022 | * |
| Elephantidae | Giraffidae | 0.0056 | ** |
| | Rhinocerotidae | 0.0017 | *** |
| Caviidae | Cervidae | 3.00E-05 | **** |
| | Equidae | 0.00053 | *** |
| | Elephantidae | 0.033 | * |
| | Giraffidae | 0.043 | * |
| | Rhinocerotidae | 0.021 | * |

**C**

| Group1 | Group2 | p.adj | p.signif |
|---|---|---|---|
| Pseudoruminant | Ruminant | 7.00E-12 | **** |
| | Hindgut | 4.40E-07 | **** |
| Ruminant | Hindgut | 3.50E-51 | **** |

Wilcoxon two-sided, adjusted p-value: *, 0.01 < p < 0.05; **, p < 0.01; ***, p < 0.001;, ****, p < 0.0001.
All pairwise comparisons not shown were not significant (p>0.05)

**Table S10.** Values of three global phylogenetic signal statistics and their associated p-values for the 37 AGF genera with significant correlations to the host phylogenetic tree*.

**Table S10. Values of three phylogenetic signal statistics and their associated p-values for the 37 AGF genera with significant correlations to the host phylogenetic tree*.**

| Genus | Phylogenetic signal statistic | | | p-values | | |
|---|---|---|---|---|---|---|
| | Abouheif's Cmean | Moran's I | Pagel's Lambda | Abouheif's Cmean | Moran's I | Pagel's Lambda |
| *Orpinomyces* | **0.21** | **0.21** | **0.60** | 0.001 | 0.001 | 0.001 |
| *Piromyces* | 0.08 | 0.09 | **0.31** | 0.001 | 0.001 | 0.001 |
| *Khyollomyces* | **0.40** | **0.40** | **0.31** | 0.001 | 0.001 | 0.001 |
| *Cyllamyces* | **0.17** | **0.16** | **0.26** | 0.001 | 0.001 | 0.001 |
| *Anaeromyces* | **0.14** | **0.13** | **0.31** | 0.001 | 0.001 | 0.001 |
| *Caecomyces* | 0.09 | 0.09 | **0.28** | 0.001 | 0.001 | 0.001 |
| *Neocallimastix* | **0.14** | **0.17** | **0.90** | 0.001 | 0.001 | 0.001 |
| *Liebetanzomyces* | 0.01 | 0.01 | **0.61** | 0.034 | 0.063 | 0.001 |
| *Paucimyces* | 0.08 | 0.09 | **0.12** | 0.001 | 0.001 | 0.001 |
| *Pecoramyces* | 0.01 | 0.02 | **0.99** | 0.035 | 0.021 | 0.001 |
| *Joblinomyces* | 0.07 | 0.07 | **0.30** | 0.002 | 0.007 | 0.001 |
| *Buwchfawromyces* | 0.01 | 0.01 | **0.10** | 0.031 | 0.038 | 1.000 |
| *Feramyces* | 0.00 | 0.00 | **0.98** | 0.037 | 0.261 | 0.001 |
| *Oontomyces* | 0.02 | 0.02 | **0.42** | 0.001 | 0.001 | 0.001 |
| NY42 | 0.05 | 0.05 | 0.06 | 0.001 | 0.003 | 0.001 |
| NY44 | **0.10** | **0.10** | **0.40** | 0.001 | 0.003 | 0.001 |
| NY1 | **0.52** | **0.95** | **1.00** | 0.001 | 0.001 | 0.001 |
| NY9 | 0.08 | 0.07 | 0.02 | 0.004 | 0.003 | 0.023 |
| NY10 | 0.01 | 0.01 | 0.07 | 0.125 | 0.128 | 0.031 |
| NY19 | 0.07 | 0.08 | **0.42** | 0.001 | 0.002 | 0.001 |
| NY53 | 0.07 | 0.07 | **0.17** | 0.001 | 0.003 | 0.001 |
| NY15 | 0.00 | 0.00 | **0.75** | 0.090 | 0.028 | 0.001 |
| NY47 | **0.10** | **0.10** | **0.21** | 0.002 | 0.004 | 0.001 |
| NY6 | 0.05 | 0.05 | 0.05 | 0.001 | 0.003 | 0.001 |
| NY7 | 0.04 | 0.04 | 0.04 | 0.002 | 0.015 | 0.002 |
| NY13 | 0.07 | 0.07 | **0.11** | 0.002 | 0.001 | 0.001 |
| NY11 | 0.00 | -0.01 | **0.99** | 0.922 | 0.965 | 0.001 |
| NY20 | 0.08 | **0.13** | **0.79** | 0.001 | 0.001 | 0.001 |
| NY17 | 0.01 | 0.01 | 0.00 | 0.019 | 0.021 | 1.000 |
| NY54 | 0.00 | 0.01 | **0.87** | 0.378 | 0.083 | 0.001 |
| AL8 | **0.24** | **0.26** | **0.61** | 0.001 | 0.001 | 0.001 |
| AL4_MN4 | **0.10** | **0.10** | **0.19** | 0.001 | 0.002 | 0.001 |
| MN3 | 0.05 | 0.05 | 0.05 | 0.003 | 0.003 | 0.001 |
| AL3 | 0.01 | 0.02 | **0.41** | 0.021 | 0.007 | 0.001 |
| RH1 | 0.08 | 0.08 | **0.12** | 0.003 | 0.003 | 0.001 |
| SK3 | **0.12** | **0.12** | **0.10** | 0.001 | 0.002 | 0.001 |
| RH2 | **0.10** | **0.13** | **0.79** | 0.001 | 0.004 | 0.001 |

* Statistic values >0.1 (as an arbitrary cutoff for correlation) are shown in boldface. Significance is shown in red font for p-values <0.05. All genera with p-value < 0.05 with at least one statistic were considered significant.

**Table S11.** Significant associations of AGF genera with studied animals based on LIPA values*. Note the high number of strong associations with hindgut animals, and the relatively lower number of strong host-AGF associations in ruminants (only in 3/22 animals: NY19 in bison, RH2 in oryx, AL8 in buffalo, NY9, SK3, and *Caecomyces* in yak, and *Neocallimastix* in elk). However, this lack of strong LIPA signal in foregut fermenters is countered by the identification of multiple intermediate and weak cophylogenetic signals (LIPA values 0.2-1; yellow in heatmap) per animal. For example, goats show intermediate and weak LIPA signals with *Joblinomyces*, NY47, and NY44, sheep show intermediate and weak LIPA signals with NY53 and *Orpinomyces*, buffaloes show intermediate and weak LIPA signals with *Cyllamyces*, NY9, NY14, and *Khoyollomyces*, bison show intermediate and weak LIPA signals with *Orpinomyces*, AL8, and RH1, oryx show intermediate LIPA signals with *Caecomyces*, *Buwchfawromyces*, and AL4/MN4, yak show weak LIPA signals with *Anaeromyces*, AL4, and *Orpinomyces*, deer show intermediate LIPA signals with *Orpinomyces*, NY13, and NY53, and elk show intermediate and weak LIPA signals with *Orpinomyces*, *Caecomyces*, *Khoyollomyces*, AL8, AL4, NY53, NY19, NY42, and NY7.

**Table S11. Significant associations of AGF genera with studied animals based on LIPA values*.**

| Gut type | Family | Animal | Strong (LIPA value>1) | Intermediate (LIPA value 0.4-1) | Weak (LIPA value 0.2-0.4) |
|---|---|---|---|---|---|
| **Ruminant** | **Giraffidae** | **Giraffe** | | *Orpinomyces* | *Khyollomyces, Cyllamyces, Anaeromyces,* NY42, NY19, NY53, AL8, AL4/MN4 |
| | **Bovidae** | **Goat** | | *Joblinomyces* , NY47 | NY44 |
| | | **Takin** | | | *Pecoramyces* |
| | | **Chamois** | | *Anaeromyces* , AL4/MN4 | *Caecomyces, Paucimyces* , NY42, NY6, NY7, AL8 |
| | | **Sheep** | | *Orpinomyces* | NY53 |
| | | **Oryx** | RH2 | *Caecomyces* , AL4/MN4, *Buwchfawromyces* | *Khyollomyces, Orpinomyces, Anaeromyces, Paucimyces,* NY6 |
| | | **Buffalo** | AL8 | *Cyllamyces* , NY9, NY14 | *Khyollomyces* |
| | | **Bison** | NY19 | *Orpinomyces* , AL8 | RH1 |
| | | **Yak** | *Caecomyces* , NY9, SK3 | | *Orpinomyces, Anaeromyces,* AL4/MN4 |
| | | **Cow** | | | *Cyllamyces, Anaeromyces,* AL8 |
| | | **Miniature Zebu** | | *Paucimyces* | |
| | **Cervidae** | **Deer** | | *Orpinomyces* , NY53, NY13 | NY6, AL4/MN4 |
| | | **Elk** | *Neocallimastix* | AL8 | *Khyollomyces, Orpinomyces, Caecomyces,* NY42, NY19, NY53, NY7, AL4/MN4 |
| **Pseudoruminant** | **Camelidae** | **Alpaca** | *Orpinomyces* , NY44 | | *Khyollomyces, Piromyces, Caecomyces, Neocallimastix, Paucimyces,* NY42, NY6, NY7 |
| | | **Camel** | *Neocallimastix, Oontomyces* | *Orpinomyces* | *Liebetanzomyces* , NY42, NY53, AL4/MN4 |
| **Hindgut** | **Caviidae** | **Capybara** | | *Orpinomyces* , AL8, AL4/MN4 | *Khyollomyces, Cyllamyces, Anaeromyces, Caecomyces,* NY53 |
| | | **Mara** | NY1, *Orpinomyces* | *Piromyces, Anaeromyces,* AL8, AL4/MN4 | *Khyollomyces, Cyllamyces, Caecomyces, Neocallimastix, Paucimyces,* NY42, NY19, NY53, NY6, NY7 |
| | **Trichechidae** | **Manatee** | *Paucimyces* , NY54 | NY6 | |
| | **Elephantidae** | **Elephant** | *Orpinomyces, Piromyces, Caecomyces* | *Anaeromyces* , AL8, AL4/MN4 | *Cyllamyces, Paucimyces,* NY42, NY19, NY53, NY6, NY7 |
| | **Equidae** | **Przewalski's Horse** | *Khyollomyces* | | *Orpinomyces* |
| | | **Horse** | *Khyollomyces* | | *Orpinomyces, Anaeromyces* |
| | | **Mule** | *Caecomyces, Orpinomyces,* AL3 | *Anaeromyces,* AL8, AL4/MN4 | *Piromyces, Cyllamyces, Neocallimastix, Paucimyces,* NY42, NY19, NY53, NY6, |
| | | **Zebra** | *Khyollomyces* | *Orpinomyces* | *Piromyces, Cyllamyces,* NY42, NY53, NY6, AL8, AL4/MN4 |
| | | **Donkey** | *Piromyces* | *Orpinomyces* | *Cyllamyces, Neocallimastix,* NY42, NY53 |
| | **Rhinocerotidae** | **Rhinoceros** | NY20 | *Orpinomyces* , AL4/MN4 | *Khyollomyces, Piromyces, Cyllamyces, Paucimyces,* NY53, NY15, AL8 |

* The following animals showed no significant association with any of the AGF genera: Okapi, Gazelle, Lechwe, Markhor, Ibex, Mountain Goat, Pere Davids Deer, Llama

**Table S12. Effect of biogeography (country of origin), age, and sex on the AGF alpha diversity in cattle, horses, goats, and sheep.** (A) ANOVA results for the effect of biogeography (country of origin), age, and sex on alpha diversity measures (Shannon, observed number of genera, Simpson, and Inverse Simpson diversity indices). Significant p-values (p-value <0.05) are shown in red text. ANOVA showed that the country of origin had a significant effect on alpha diversity in cattle (with all indices, p-value <0.03), horses (with 3 out of 4 indices, p-value <0.04), but not in goats (with 3 out of 4 indices, p-value >0.1), or sheep (with 3 out of 4 indices, p-value >0.05). On the other hand, animal sex largely had no significant effect on alpha diversity (p-value>0.05). Animal age only showed a significant effect on the alpha diversity of horses (with all indices, p-value <0.03), goats (with all indices, p-value <0.01), and sheep (with 2 out of 4 indices, p-value <0.003), but not cattle. Since out of the three non-host associated factors tested, biogeography showed the most significant effect on alpha diversity, we further carried out Tukey HSD tests for pairwise country (B), and US state (C) comparisons for the two animals with the most significant results (cattle and horses). Cattle samples from the USA, and New Zealand were found to be more diverse than cattle from Germany, but no significant difference was observed in alpha diversity of cattle from all other countries. Similarly, horse samples from USA were found to be more diverse than horses from Germany. Within the USA, the state of origin significantly affected the alpha diversity in cattle, and horses. Analysis of variance showed only significantly higher diversity in cattle originating from OK, in comparison to AZ, CT, and FL, and significantly higher diversity in horses originating from OK, in comparison to CT.

**A**

| Animal Genus | ANOVA p-value | | | | Factor |
|---|---|---|---|---|---|
| | Observed Genera | Shannon | Simpson | InvSimpson | |
| Cattle | 5.35E-05 | 0.0007 | 0.028 | 0.014 | Biogeography |
| | 0.59 | 0.64 | 0.81 | 0.80 | Age |
| | 0.29 | 0.63 | 0.33 | 0.32 | Sex |
| Horses | 0.074 | 0.0006 | 0.0012 | 0.038 | Biogeography |
| | 0.025 | 0.0026 | 0.02 | 0.018 | Age |
| | 0.48 | 0.15 | 0.09 | 0.091 | Sex |
| Goats | 0.56 | 0.82 | 0.78 | 0.042 | Biogeography |
| | 1.5E-05 | 9.8E-05 | 0.0065 | 0.007 | Age |
| | 0.026 | 0.057 | 0.09 | 0.095 | Sex |
| Sheep | 0.0003 | 0.057 | 0.59 | 0.6 | Biogeography |
| | 7E-05 | 0.0002 | 0.3 | 0.32 | Age |
| | 0.006 | 0.0008 | 0.7 | 0.73 | Sex |

**B**

| Animal Genus | Countries compared | | HSD Tukey p-value | | | |
|---|---|---|---|---|---|---|
| | | | Observed genera | Shannon | Simpson | InvSimpson |
| Cattle | New Zealand | Germany | 0.039 | 0.022 | 0.036 | 0.032 |
| | USA | Germany | 0.00003 | 0.001 | 0.072 | 0.053 |
| Horses | USA | Germany | 0.12 | 0.0028 | 0.004 | 0.14 |

**C**

| Animal Genus | USA states compared | | HSD Tukey p-value | | | |
|---|---|---|---|---|---|---|
| | | | Observed genera | Shannon | Simpson | InvSimpson |
| Cattle | Oklahoma | Arizona | 0 | 0.00005 | 0.0076 | 0.051 |
| | Oklahoma | Connecticut | 0.76 | 0.012 | 0.0008 | 0.32 |
| | Oklahoma | Florida | 0 | 0.0002 | 0.0067 | 0.12 |
| Horses | Oklahoma | Connecticut | 0.48 | 0.000002 | 0.0000006 | 0.03 |

**Table S13. Results of metagenomic sequencing of the 9 selected samples. Shown are the number of reads and total number of bases before and after quality trimming.**

| Sample name | Animal | Sequencing output | | Following quality trimming | |
|---|---|---|---|---|---|
| | | Number of reads | Total number of bases | Number of reads | Total number of bases |
| Cow 121 | Cattle | 83,926,834 | 25,261,977,034 | 80,901,766 | 21,031,553,774 |
| Goat Lgoat 25 2 | Goat | 72,673,118 | 21,874,608,518 | 68,489,562 | 17,562,335,438 |
| Sheep 471 | Sheep | 84,196,164 | 25,343,045,364 | 79,923,682 | 20,659,377,046 |
| Deer 526 | Deer | 66,695,652 | 20,075,391,252 | 65,036,454 | 15,804,516,149 |
| Elephant zoo 499 | Elephant | 73,457,424 | 22,110,684,624 | 70,292,190 | 17,915,763,157 |
| Horse 168 | Horse | 77,726,102 | 23,395,556,702 | 74,814,616 | 19,119,611,975 |
| Camel zoo 839 | Camel | 57,559,998 | 17,325,559,398 | 54,912,228 | 14,055,855,640 |
| Buffalo Egypt E76 | Buffalo | 42,362,582 | 12,751,137,182 | 39,129,976 | 9,782,563,439 |
| Bison Zoo 597 | Bison | 80,459,672 | 24,218,361,272 | 77,591,290 | 18,562,869,841 |

**Table S14. Read assembly results using IDBA-UD for the 9 samples sequenced.**

| Sample name | Animal | Total number of contigs | No. of contigs > 10,000 bp | No. of contigs > 100,000 bp | Largest contig (bp) | Total length (bp) | N50 | L50 | GC (%) |
|---|---|---|---|---|---|---|---|---|---|
| Cow_121 | Cattle | 22,543 | 1512 | 12 | 186,390 | 106,443,704 | 5,127 | 4,599 | 44.09 |
| Goat_Lgoat_25_2 | Goat | 37,605 | 6488 | 108 | 402,076 | 288,827,951 | 12,265 | 5,020 | 46.03 |
| Sheep_471 | Sheep | 26,307 | 1606 | 7 | 229,995 | 116,917,695 | 4,589 | 5,748 | 43.78 |
| Deer_526 | Deer | 17,703 | 1849 | 7 | 142,102 | 101,222,234 | 7,179 | 2,888 | 48.28 |
| Elephant_zoo_499 | Elephant | 56,833 | 4620 | 8 | 157,691 | 283,652,401 | 5,654 | 12,544 | 46.29 |
| Horse_168 | Horse | 32,942 | 1707 | 7 | 165,452 | 141,971,471 | 4,455 | 8,103 | 46.56 |
| Camel_zoo_839 | Camel | 24,891 | 2889 | 21 | 263,806 | 145,931,569 | 7,834 | 4,001 | 42.65 |
| Buffalo_Egypt_E76 | Buffalo | 7,448 | 310 | 2 | 116,491 | 30,156,346 | 4,013 | 1,918 | 45.27 |
| Bison_Zoo_597 | Bison | 28,642 | 2644 | 12 | 171,965 | 152,314,276 | 6,266 | 5,461 | 44.3 |

**Table S15.** Results of eukaryotic contigs identification using EukRep, and binning using CONCOCT. For bins >1M bp, the GC content and the taxonomic classification using the prokaryotic classifier GTDB-Tk are shown. All bins larger than 1M bp were classified as bacterial with a GC content ≥38%.

| Sample name | Animal | EukRep contigs | Binned contigs | Total Number of bins | Bins >1M bp | | |
|---|---|---|---|---|---|---|---|
| | | | | | Number of bins | GC content | GTDB taxonomy (Class level) |
| Cow_121 | Cattle | 3025 | 2071 | 58 | 3 | 47.1, 47, 39.8 | Bacteroidia |
| Goat_Lgoat_25_2 | Goat | 2131 | 1621 | 23 | 2 | 57.3, 39.7 | Clostridia, Bacilli |
| Sheep_471 | Sheep | 2756 | 1888 | 67 | 4 | 38.6, 41.3, 42.8, 46.4 | 3 Bacteroidia, 1 Clostridia |
| Deer_526 | Deer | 1793 | 1226 | 23 | 1 | 52.3 | Clostridia |
| Elephant_zoo_499 | Elephant | 5443 | 3972 | 56 | 5 | 43.6, 60.4, 39.4, 36.7, 47.7 | 2 Bacteroidia, 1 Kiritimatiellae, 2 Clostridia |
| Horse_168 | Horse | 3469 | 2310 | 51 | 4 | 41.6, 56.4, 45.6, 45 | 3 Bacteroidia, 1 Kiritimatiellae |
| Camel_zoo_839 | Camel | 1917 | 1379 | 36 | 1 | 44.5 | Bacteroidia |
| Buffalo_Egypt_E76 | Buffalo | 869 | 529 | 21 | 1 | 42.1 | Clostridia |
| Bison_Zoo_597 | Bison | 2864 | 2118 | 46 | 3 | 42.6, 45, 43.8 | Bacteroidia, Clostridia, Bacilli |

**Table S16.** Previous metagenomic studies conducted on herbivorous gut microbiome. Only one study (that employed a deep sequencing strategy (>1 Tbp of data), successfully recovered AGF genomic contigs.

| Study animal | Reference | NCBI BioProject ID | Notes |
|---|---|---|---|
| Metagenomic sequencing of the GIT of ruminants | [52] | PRJNA657455, PRJNA657473 | This study produced a total of 6.5 terabytes (Tb) of high quality data, and identified 13 bins belonging to AGF from a total of 28,543 metagenome-assembled genomic bins. These AGF bins were fragmented and only represented <1% of their respective reference genome. |
| Metagenomic sequencing of African cattle rumen | [53] | PRJEB39057 | No AGF reads/ contigs/ bins were identified. |
| Metagenomic sequencing of bovine rumen | [54] | PRJEB23561 | No AGF reads/ contigs/ bins were identified. |
| Metagenomic sequencing of the Caprinae gut microbiota | [55] | PRJCA008889 | No AGF reads/ contigs/ bins were identified. |
| Metagenomic sequencing of the large intestine of domesticated cattle | [56] | PRJNA681986 | No AGF reads/ contigs/ bins were identified. |
| Metagenomic sequencing of the cow rumen | [57] | PRJEB21624 | No AGF reads/ contigs/ bins were identified. |
| Metagenomic sequencing of 283 ruminant cattle | [58] | PRJEB31266 and PRJEB21624. | No AGF reads/ contigs/ bins were identified. |
| Metagenomic sequencing of camel gut | [59] | PRJNA746430 | No AGF reads/ contigs/ bins were identified. |
| Metagenomic sequencing of different fractions of the cow rumen | [60] | PRJEB47520 | No AGF reads/ contigs/ bins were identified. |
| Metagenomic sequencing of samples from six intestinal regions of dairy cows | [61] | PRJNA723218 | No AGF reads/ contigs/ bins were identified. |
| Metagenomic sequencing of capybara gut microbiome | [62] | PRJNA563062. | No AGF reads/ contigs/ bins were identified. |
| Rumen microbiome of cattle in Japan | [63] | PRJDB13503 | No AGF reads/ contigs/ bins were identified. |
| Metagenomic sequencing of the beef cattle rumen | [64] | PRJEB10338 and PRJEB31266 | No AGF reads/ contigs/ bins were identified. |
| Metagenomic sequencing of cattle, sheep, moose, deer, and bison gut microbiomes | [65] | PRJNA627299 and PRJNA627251 | No AGF reads/ contigs/ bins were identified. |
| Metagenomic sequencing of rumen-fistulated moose | [66] | PRJNA301235 | No AGF reads/ contigs/ bins were identified. |
| Metagenomic sequencing of the dairy cattle rumen | [67] | PRJNA526070 and PRJNA597489 | No AGF reads/ contigs/ bins were identified. |
| Metagenomic sequencing of Colombian buffalos' gut microbiome | [68] | PRJNA605425 | No AGF reads/ contigs/ bins were identified. |

| | | | |
|---|---|---|---|
| Metagenomic sequencing of the cow, sheep, reindeer and red deer rumen | [69] | PRJEB34458 | No AGF reads/ contigs/ bins were identified. |
| Metagenomic sequencing of cattle rumen | [70] | PRJNA631951 | No AGF reads/ contigs/ bins were identified. |
| Metagenomic sequencing of the yak fecal microbial community | [71] | PRJNA624740 | No AGF reads/ contigs/ bins were identified. |
| Metagenomic sequencing of the equine fecal microbiome | [72] | PRJNA590977 | No AGF reads/ contigs/ bins were identified. |
| Metagenomic Sequencing of sheep cecal microbiota | [73] | PRJNA702231 | No AGF reads/ contigs/ bins were identified. |
| Metagenomic sequencing of the equine gut microbiome | [74] | PRJNA438436 | No AGF reads/ contigs/ bins were identified. |
| Metagenomic sequencing of samples enriched using cow rumen and sugarcane bagasse | [75] | PRJEB30762 | No AGF reads/ contigs/ bins were identified. |
| Metagenomic sequencing of the moose (Alces alces) rumen | [76] | PRJEB12797 | No AGF reads/ contigs/ bins were identified. |
| Metagenomic sequencing of the gastrointestinal microbiome in dairy cattle | [77] | PRJNA723218 | No AGF reads/ contigs/ bins were identified. |
| Metagenomic sequencing of the microbiome of the buffalo digestive tract | [78] | PRJNA656389 | No AGF reads/ contigs/ bins were identified. |
| Metagenomic sequencing of goats' gut microbiome | [79] | PRJNA792486 | No AGF reads/ contigs/ bins were identified. |
| Metagenomic sequencing of the dairy cattle rumen | [80] | PRJNA883555 | No AGF reads/ contigs/ bins were identified. |

**References**


1. Mahayri TM*, et al.* Host species affects bacterial evenness, but not diversity: Comparison of fecal bacteria of cows and goats offered the same diet. *Animals* **12**, 2011 (2022).

2. Dagar SS, Kumar S, Mudgil P, Singh R, Puniya AK. D1/D2 Domain of Large-Subunit Ribosomal DNA for Differentiation of Orpinomyces spp. *Appl Environ Microbiol* **77**, (2011).

3. Hanafy RA, Johnson B, Youssef NH, Elshahed MS. Assessing anaerobic gut fungal diversity in herbivores using D1/D2 large ribosomal subunit sequencing and multi-year isolation. *Environ Microbiol* **22**, 3883-3908 (2020).

4. Elshahed MS*, et al.* Characterization and rank assignment criteria for the anaerobic fungi (Neocallimastigomycota). *Int J Syst Evol Microbiol* **72**, doi: 10.1099/ijsem.1090.005449. (2022).

5. Hanafy RA, Johnson B, Youssef NH, Elshahed MS. Assessing anaerobic gut fungal diversity in herbivores using D1/D2 large ribosomal subunit sequencing and multi-year isolation. *Environ Microbiol* **22**, 3883-3908 (2020).

6. Edwards JE, Hermes GDA, Kittelmann S, Nijsse B, Smidt H. Assessment of the accuracy of high-throughput sequencing of the ITS1 region of Neocallimastigomycota for community composition analysis. *Front Micorobiol* **10**, 2370 (2019).

7. Young D*, et al.* Simultaneous metabarcoding and quantification of Neocallimastigomycetes from environmental samples: Insights into community composition and novel lineages. *Microorganisms* **10**, 1749 (2022).

8. Nagler M, Podmirseg SM, Griffith GW, Insam H, Ascher-Jenull J. The use of extracellular DNA as a proxy for specific microbial activity. *Appl Microbiol Biotechnol* **102**, 2885-2898 (2018).

9. Schloss PD*, et al.* Introducing mothur: open-source, platform-independent, community-supported software for describing and comparing microbial communities. *Appl Environ Microbiol* **75**, 7537-7541 (2009).

10. Price MN, Dehal PS, Arkin AP. FastTree 2--approximately maximum-likelihood trees for large alignments. *PLoS One* **5**, e9490 (2010).

11. Minh BQ*, et al.* IQ-TREE 2: new models and efficient methods for phylogenetic inference in the genomic era. *Mol Biol Evol* **37**, 1530-1534 (2020).

12. Kalyaanamoorthy S, Minh BQ, Wong TKF, von Haeseler A, Jermiin LS. ModelFinder: fast model selection for accurate phylogenetic estimates. *Nature Methods* **14**, 587-589 (2017).

13. Hoang DT, Chernomor O, von Haeseler A, Minh BQ, Vinh LS. UFBoot2: Improving the ultrafast bootstrap approximation. *Mol Biol Evol* **35**, 518-522 (2018).

14. García-López R*, et al.* OTUs and ASVs produce comparable taxonomic and diversity from shrimp microbiota 16S profiles using tailored abundance filters. *Genes* **12**, 564 (2021).

15. Wolfgang A*, et al.* Understanding the impact of cultivar, seed origin, and substrate on bacterial diversity of the sugar beet rhizosphere and suppression of soil-borne pathogens. *Front Plant Sci* **11**, 560869 (2020).

16. Inkinen J*, et al.* Diverse and active archaea communities occur in non-disinfected drinking water systems–Less activity revealed in disinfected and hot water systems. *Water Res X* **12**, 100101 (2021).

17. de Souza LMD*, et al.* Diversity, distribution and ecology of fungal communities present in Antarctic lake sediments uncovered by DNA metabarcoding. *Sci Rep* **12**, 8407 (2022).

18. Callahan BJ, McMurdie PJ, Holmes SP. Exact sequence variants should replace operational taxonomic units in marker-gene data analysis. *ISME J* **11**, 2639-2643 (2017).

19. Caruso V, Song X, Asquith M, Karstens L. Performance of microbiome sequence inference methods in environments with varying biomass. *mSystems* **4**, e00163-00118 (2019).

20. Fricker AM, Podlesny D, Fricke WF. What is new and relevant for sequencing-based microbiome research? A mini-review. *J Adv Res* **19**, 105-112 (2019).

21. Joos L*, et al.* Daring to be differential: metabarcoding analysis of soil and plant-related microbial communities using amplicon sequence variants and operational taxonomical units. *BMC Genomics* **21**, 733 (2020).

22. Ning D, Deng Y, Tiedje JM, Zhou J. A general framework for quantitatively assessing ecological stochasticity. *Proc Natl Acad Sci USA* **116**, 16892-16898 (2019).

23. Stegen JC, Lin X, Fredrickson JK, Konopka AE. Estimating and mapping ecological processes influencing microbial community assembly. *Front Microbiol* **6**, 370 (2015).

24. Zhou J, Ning D. Stochastic community assembly: Does It matter in microbial ecology? *Microbiol Mol Biol Rev* **81**, e00002-00017 (2017).

25. Anderson MJ, Walsh DCI. PERMANOVA, ANOSIM, and the Mantel test in the face of heterogeneous dispersions: What null hypothesis are you testing? *Ecol Monographs* **83**, 557-574 (2013).

26. Youngblut ND*, et al.* Vertebrate host phylogeny influences gut archaeal diversity. *Nat Microbiol* **6**, 1443-1454 (2021).

27. Murphy CL*, et al.* Horizontal gene transfer forged the evolution of anaerobic gut fungi into a phylogenetically distinct gut-dwelling fungal lineage. . *Appl Environ Microbiol* **85**, e00988-00919 (2019).

28. Wang Y, Youssef NH, Couger MB, Hanafy RA, Elshahed MS, Stajich JE. Molecular dating of the emergence of anaerobic rumen fungi and the impact of laterally acquired genes. *mSystems* **4**, e00247-00219 (2019).

29. Hanafy RA*, et al.* Seven new Neocallimastigomycota genera from wild, zoo-housed, and domesticated herbivores greatly expand the taxonomic diversity of the phylum. . *Mycologia 112, :1212-1239 (2020).*

30. Gruninger RJ*, et al.* Application of transcriptomics to compare the carbohydrate active enzymes that are expressed by diverse genera of anaerobic fungi to degrade plant cell wall carbohydrates. *Front Microbiol* **9**, 1581 (2018).

31. Haitjema CH*, et al.* A parts list for fungal cellulosomes revealed by comparative genomics. *Nature Microbiol* **2**, 17087 (2017).

32. Wilken SE*, et al.* Experimentally validated reconstruction and analysis of a genome-scale metabolic model of an anaerobic Neocallimastigomycota fungus. *mSystems* **16**, e00002-00021 (2021).

33. Li Y*, et al.* Combined genomic, transcriptomic, proteomic, and physiological characterization of the growth of *Pecoramyces* sp. F1 in monoculture and co-culture with a syntrophic methanogen. *Front Microbiol* **10**, 435 (2019).

34. Calkins S, Elledge NC, Hanafy RA, Elshahed MS, Youssef N. A fast and reliable procedure for spore collection from anaerobic fungi: Application for RNA uptake and long-term storage of isolates. *J Microbiol Meth* **127**, 206-213 (2016).

35. Fu L, Niu B, Zhu Z, Wu S, Li W. CD-HIT: accelerated for clustering the next-generation sequencing data. *Bioinformatics* **28**, 3150-3152 (2012).

36. Manni M, Berkeley MR, Seppey M, Simão FA, Zdobnov EM. BUSCO Update: Novel and Streamlined Workflows along with Broader and Deeper Phylogenetic Coverage for Scoring of Eukaryotic, Prokaryotic, and Viral Genomes. *Mol Biol Evol* **38**, 4647-4654 (2021).

37. Hanafy RA, Wang Y, Stajich JE, Pratt CJ, Youssef NH, Elshahed MH. Phylogenomic analysis of the Neocallimastigomycota: proposal of *Caecomycetaceae* fam. nov., *Piromycetaceae* fam. nov., and emended description of the families *Neocallimastigaceae* and *Anaeromycetaceae*. *Int J Syst Evol Microbiol* **273**, https://doi.org/10.1099/ijsem.1090.005735 (2023).

38. Capella-Gutiérrez S, Silla-Martínez JM, Gabaldón T. trimAl: a tool for automated alignment trimming in large-scale phylogenetic analyses. *Bioinformatics* **25**, 1972-1973 (2009).

39. Lanfear R, Frandsen PB, Wright AM, Senfeld T, Calcott B. PartitionFinder 2: new methods for selecting partitioned models of evolution for molecular and morphological phylogenetic analyses. *Mol Biol Evol* **34**, 772-773 (2016).

40. Suchard MA, Lemey P, Baele G, Ayres DL, Drummond AJ, Rambaut A. Bayesian phylogenetic and phylodynamic data integration using BEAST 1.10. *Virus Evol* **4**, vey016 (2018).

41. Rambaut A, Drummond AJ, Xie D, Baele G, Suchard MA. Posterior summarization in Bayesian phylogenetics using Tracer 1.7. *Syst Biol* **67**, 901-904 (2018).

42. Bolger AM, Lohse M, Usadel B. Trimmomatic: a flexible trimmer for Illumina sequence data. *Bioinformatics* **30**, 2114-2120 (2014).

43. Menzel P, Ng KL, Krogh A. Fast and sensitive taxonomic classification for metagenomics with Kaiju. *Nat Commun* **7**, 11257 (2016).

44. Peng Y, Leung HC, Yiu SM, Chin FY. IDBA-UD: a de novo assembler for single-cell and metagenomic sequencing data with highly uneven depth. *Bioinformatics* **28**, 1420-1428 (2012).

45. West PT, Probst AJ, Grigoriev IV, Thomas BC, Banfield JF. Genome-reconstruction for eukaryotes from complex natural microbial communities. *Genome Res* **28**, 569-580 (2018).

46. Alneberg J*, et al.* Binning metagenomic contigs by coverage and composition. *Nature Methods* **11**, 1144-1146 (2014).

47. Chaumeil P-A, Mussig AJ, Hugenholtz P, Parks DH. GTDB-Tk v2: memory friendly classification with the genome taxonomy database. *Bioinformatics* **38**, 5315-5316 (2022).

48. Allen B, Drake M, Harris N, Sullivan T. Using KBase to assemble and annotate prokaryotic genomes. *Curr Protoc Microbiol* **46**, 1e.13.11-11e.13.18 (2017).

49. Arkin AP*, et al.* KBase: The United States Department of Energy systems biology knowledgebase. *Nat Biotechnol* **36**, 566-569 (2018).

50. Chivian D*, et al.* Metagenome-assembled genome extraction and analysis from microbiomes using KBase. *Nat Protoc* **18**, 208-238 (2023).

51. Wang Y, Qian PY. Conservative fragments in bacterial 16S rRNA genes and primer design for 16S ribosomal DNA amplicons in metagenomic studies. *PLoS One* **4**, e7401 (2009).

52. Xie F*, et al.* An integrated gene catalog and over 10,000 metagenome-assembled genomes from the gastrointestinal microbiome of ruminants. *Microbiome* **9**, 137 (2021).

53. Wilkinson T*, et al.* 1200 high-quality metagenome-assembled genomes from the rumen of African cattle and their relevance in the context of sub-optimal feeding. *Genome Biol* **21**, 229 (2020).

54. Li J*, et al.* A catalog of microbial genes from the bovine rumen unveils a specialized and diverse biomass-degrading environment. *Gigascience* **9**, (2020).

55. Zhang XX*, et al.* A catalog of over 5,000 metagenome-assembled microbial genomes from the Caprinae gut microbiota. *Microbiol Spectr* **10**, e0221122 (2022).

56. Teseo S*, et al.* A global phylogenomic and metabolic reconstruction of the large intestine bacterial community of domesticated cattle. *Microbiome* **10**, 155 (2022).

57. Stewart RD*, et al.* Assembly of 913 microbial genomes from metagenomic sequencing of the cow rumen. *Nat Commun* **9**, 870 (2018).

58. Stewart RD, Auffret MD, Warr A, Walker AW, Roehe R, Watson M. Compendium of 4,941 rumen metagenome-assembled genomes for rumen microbiome biology and enzyme discovery. *Nat Biotechnol* **37**, 953-961 (2019).

59. Gharechahi J, Sarikhan S, Han JL, Ding XZ, Salekdeh GH. Functional and phylogenetic analyses of camel rumen microbiota associated with different lignocellulosic substrates. *NPJ Biofilms Microbiomes* **8**, 46 (2022).

60. Hernández R, Chaib De Mares M, Jimenez H, Reyes A, Caro-Quintero A. Functional and phylogenetic characterization of bacteria in bovine rumen using fractionation of ruminal fluid. *Front Microbiol* **13**, 813002 (2022).

61. Lin L*, et al.* Genome-centric investigation of bile acid metabolizing microbiota of dairy cows and associated diet-induced functional implications. *ISME J* **17**, 172-184 (2023).

62. Cabral L*, et al.* Gut microbiome of the largest living rodent harbors unprecedented enzymatic systems to degrade plant polysaccharides. *Nat Commun* **13**, 629 (2022).

63. Sato Y*, et al.* Identification of 146 Metagenome-assembled Genomes from the Rumen Microbiome of Cattle in Japan. *Microbes Environ* **37**, (2022).

64. Auffret MD, Stewart RD, Dewhurst RJ, Duthie CA, Watson M, Roehe R. Identification of microbial genetic capacities and potential mechanisms within the rumen microbiome explaining differences in beef cattle feed efficiency. *Front Microbiol* **11**, 1229 (2020).

65. Anderson CL, Fernando SC. Insights into rumen microbial biosynthetic gene cluster diversity through genome-resolved metagenomics. *Commun Biol* **4**, 818 (2021).

66. Solden LM*, et al.* Interspecies cross-feeding orchestrates carbon degradation in the rumen ecosystem. *Nat Microbiol* **3**, 1274-1284 (2018).

67. Xue MY*, et al.* Investigation of fiber utilization in the rumen of dairy cows based on metagenome-assembled genomes and single-cell RNA sequencing. *Microbiome* **10**, 11 (2022).

68. Aguilar-Marin SB, Betancur-Murillo CL, Isaza GA, Mesa H, Jovel J. Lower methane emissions were associated with higher abundance of ruminal Prevotella in a cohort of Colombian buffalos. *BMC Microbiol* **20**, 364 (2020).

69. Glendinning L, Genç B, Wallace RJ, Watson M. Metagenomic analysis of the cow, sheep, reindeer and red deer rumen. *Sci Rep* **11**, 1990 (2021).

70. Gharechahi J, Vahidi MF, Bahram M, Han JL, Ding XZ, Salekdeh GH. Metagenomic analysis reveals a dynamic microbiome with diversified adaptive functions to utilize high lignocellulosic forages in the cattle rumen. *ISME J* **15**, 1108-1120 (2021).

71. Gong G, Zhou S, Luo R, Gesang Z, Suolang S. Metagenomic insights into the diversity of carbohydrate-degrading enzymes in the yak fecal microbial community. *BMC Microbiol* **20**, 302 (2020).

72. Gilroy R*, et al.* Metagenomic investigation of the equine faecal microbiome reveals extensive taxonomic diversity. *PeerJ* **10**, e13084 (2022).

73. Xie F, Xu L, Wang Y, Mao S. Metagenomic sequencing reveals that high-grain feeding alters the composition and metabolism of cecal microbiota and induces cecal mucosal injury in sheep. *mSystems* **6**, e0091521 (2021).

74. Mach N*, et al.* Mining the equine gut metagenome: poorly-characterized taxa associated with cardiovascular fitness in endurance athletes. *Commun Biol* **5**, 1032 (2022).

75. Tomazetto G, Pimentel AC, Wibberg D, Dixon N, Squina FM. Multi-omic directed discovery of cellulosomes, polysaccharide utilization loci, and lignocellulases from an enriched rumen anaerobic consortium. *Appl Environ Microbiol* **86**, (2020).

76. Svartström O*, et al.* Ninety-nine de novo assembled genomes from the moose (Alces alces) rumen microbiome provide new insights into microbial plant biomass degradation. *ISME J* **11**, 2538-2551 (2017).

77. Lin L, Lai Z, Zhang J, Zhu W, Mao S. The gastrointestinal microbiome in dairy cattle is constrained by the deterministic driver of the region and the modified effect of diet. *Microbiome* **11**, 10 (2023).

78. Tong F*, et al.* The microbiome of the buffalo digestive tract. *Nat Commun* **13**, 823 (2022).

79. Zhang T*, et al.* Transmission of the gut microbiome in cohousing goats and pigs. *Front Microbiol* **13**, 948617 (2022).

80. Zhang L, Shen H, Zhang J, Mao S. Variety of rumen microbial populations involved in biohydrogenation related to individual milk fat percentage of dairy cows. *Front Vet Sci* **10**, 1106834 (2023).